Supplementary Materials for

Title: Aibp-mediated Cholesterol Efflux Instructs Hematopoietic Stem and Progenitor Cell Fate

Qilin Gu[1], Xiaojie Yang[1*], Jie Lv[1,2*], Jiaxiong Zhang[1,3*], Bo Xia[1,2], Jun-dae Kim[1], Ruoyu Wang[4,5], Feng Xiong[4], Shu Meng[1], Thomas P. Clements[6], Bhavna Tandon[6], Daniel S. Wagner[6], Miguel F. Diaz[7], Pamela L. Wenzel[7], Yury I. Miller[8], David Traver[9], John P. Cooke[1,10,11], Wenbo Li[4,5], Leonard I. Zon[12], Kaifu Chen[1,2,10,11†], Yongping Bai[3†], Longhou Fang[1,10,11,13†]

*Corresponding author: to Longhou Fang, Department of Cardiovascular Sciences, Houston Methodist Research Institute, Houston, Texas 77030, USA.
Email: lhfang@houstonmethodist.org,

to Yongping Bai, Department of Geriatric Medicine, Xiangya Hospital, Central South University, Changsha, China. Email: baiyongping@csu.edu.cn,

or Kaifu Chen, Department of Cardiovascular Sciences, Houston Methodist Research Institute, Houston, Texas 77030, USA. Email: kchen2@houstonmethodist.org.

This PDF file includes:

contributed to human blood collection and data analysis; R.W. and F. X. contributed to ATAC-seq library generation and sequencing. L.Z., D.T, J.C and P.W provided constructive suggestions and experimental materials. D.W., P.W., W.L., Y.M., D.T., J.C., L.Z., K.C., Y.B. and L.F. critically revised the manuscript.

Materials and Methods

Animal husbandry

Zebrafish lines and *Ldlr*$^{-/-}$ (B6) mice were maintained as previously described (*25, 26*) and in accordance with Houston Methodist Research Institute Animal Care and Use Committee (IACUC) regulations and under the appropriate project protocols.

Generation of transgenic zebrafish lines

Tg(kdrl:Gal4ER^{T2}*)*: a 6.8 kb fragment of *kdrl* promoter/enhancer sequence, which drives EC-specific gene expression (*10*), was cloned and replaced the ubiquitin promoter in the *ubiquitin:Gal4ER*^{T2}*-ACR* vector (*27*) using primers (kdrl-F: 5'-TTGTTTAAGCTTGA TAAGCTTTTTCTTTTTTATTTAAAATTAAATGTAATAC-3'; kdrl-R: 5'- CACCGG CCATGTCGATTTGTCTGTTAAAATAACGTCCCGAATG-3'). *Tg(UAS:Flag-nSrebp2-2A-mCerulean3)*: a PCR-amplified *mCerulean3* (Addgene plasmid, #54730) was used to replace the EGFP site in the *pBT2-4×UAS:EGFP* vector (Halpern Lab #744) to generate *pBT2-4×UAS:mCerulean3* vector. The 2A (5'-GCTACTAACTTCAGCCT GCTGAAGCAGGCTGGAGACGTGGAGGAGAACCCTGGACCT-3') sequence was cloned in-frame upstream of *mCerulean3* to generate *pBT2-4×UAS:2A-mCerulean3* vector. The NH_2-terminal segment of zebrafish Srebp2 (460aa) was ligated in-frame with 2A-*mCerulean3*. To generate *Tg(UAS:NICD-2A-mRFP)*, a PCR-amplified 2A-mRFP from *pCS2-SmaI-2A-mRFP* was cloned to replace EGFP site in the *pBT2-4×UAS:GFP* vector to generate the *pBT2-4×UAS:2A-mRFP* vector. The zebrafish Notch intracellular domain (NICD) (*28*) was inserted in-frame into the upstream of the 2A-mRFP to create the *pBT2-4×UAS:NICD-2A-mRFP* vector. All plasmids had a mini Tol2 element to facilitate genomic integration in zebrafish. One-cell stage zebrafish embryos were microinjected with 25 pg of the final transgenic DNA construct along with 50 pg *Tol2 transposase* mRNA. Positive F0 founders were backcrossed with wild-type AB zebrafish and F1 offspring were further screened to assess germline transmission. Positive founder lines were identified according to mCerulean3 or mRFP expression in F1 larvae treated with 4OHT. F1 zebrafish were used to generate embryos for all experiments described.

MO and mRNA injections

Morpholino antisense oligos (MOs) used in this study were synthesized by Gene Tools. The MO sequences are: Control: 5'- CCTCTTACCTCAGTTACAATTTATA-3', *apoa1bp2* (NCBI Gene ID: 557840): 5'-GTGGTTCATCTTGATTTATTCGGC-3' (*5*), *srebf2* (NCBI Gene ID: 100037309) MO: 5'-TCCATGTTTCTCCACCTTCTCTC-3'. MO were diluted in RNase-free water, and then mixed with RNase-free phenol Red solution to achieve a concentration of 0.2 mM (control MO), 0.1 mM (*apoa1bp2* MO) or 0.2 mM (*srebf2* MO). For mRNA injection, equal volume of MO and mRNA were mixed to make a final concentration of 100-150 ng/μl *apoa1bp2* or transcriptionally active N-terminal *srebf2* mRNA with 0.1 mM *apoa1bp2* MO or 0.2 mM *srebf2* MO, respectively. Each one-cell stage embryo was injected with 1 nl MO or MO in combination with

mRNA using a microinjector FemtoJet® 4i (Eppendorf).

Aibp2 antibody injection

Zebrafish antibody injection was performed as previously described (*29*). Briefly, one-cell stage zebrafish embryos were collected and 1 nl of heat-inactivated (30 min at 72°C) zebrafish Aibp2 antibody (*1*), or normal Aibp2 antibody (30 min at room temperature) were injected. The resulting embryos were raised to the indicated stages for whole mount in situ hybridization analysis.

CRISPR/Cas9-mediated gene ablation

The CRISPR/Cas9-mediated gene disruption method in zebrafish was conducted as previously described (*30*). The target sequences for *apoa1bp2* and *srebf2* were 5'-TGTTGAGACGGAGCTCCTGA-3' and 5'-GCCCGTGGGGCTCTGGACAG-3', respectively. In brief, 2 μl of each of the two complementary target oligonucleotides (100 μM) was annealed by incubating the mixture at 95°C for 5 min, and the annealed oligos were then inserted into the pT7-gRNA vector. The linearized template DNA was used for guide-RNA (gRNA) synthesis using HiScribe™ T7 Quick High Yield RNA Synthesis (New England Biolabs). The gRNA was purified using *mir*Vana miRNA isolation kit (Invitrogen), and the size and quality of resulting gRNA was confirmed by electrophoresis through a 2% (wt/vol) formaldehyde agarose gel. The pCS2-nCas9n was linearized and capped nls-zCas9-nls RNA was synthesized using mMESSAGE mMACHINE SP6 kit (Invitrogen). The gRNA (25 ng/μl) and Cas9 RNA (200 ng/μl) mixture was injected into one-cell stage WT (AB) embryos. At 5 dpf, genomic DNA of the resulting embryos was prepared using Genomic DNA extraction kit (Zymo Research). A short genomic region flanking the target site was PCR amplified from the genomic DNA. The PCR amplicons were purified using QIAquick PCR Purification kit (Qiagen), and a total of 200 ng of the purified PCR products were denatured and reannealed to facilitate heteroduplex formation. The reannealed amplicon was then digested with 1 units of T7 endonuclease I (New England Biolabs) at 37 °C for 4 hr. The samples were then resolved by agarose gel electrophoresis (2-2.5%) and visualized by Gel red staining. The F0 animals were crossed with AB zebrafish to obtain F1. To assess genetic disruption, the target region in F1 animals was PCR amplified and the resulting amplicons were cloned into pMD20 TA vector (Clontech). The plasmids of the resulting colonies were isolated and sequenced.

Chemical treatments

Four-hydroxy-tamoxifen (4OHT) (H7904, Sigma) was dissolved in ethanol at 10 mM and stored at -20°C. Embryos were incubated with 5 μM of 4OHT or equal amount of control vehicle (ethanol) in E3 medium (5 mM NaCl, 0.17 mM KCl, 0.33 mM $CaCl_2$, 0.33 mM $MgSO_4$ and 0.1% methylene blue) from 6 to 26 hpf. Atorvastatin (PZ0001, Sigma) was dissolved to a concentration of 2 mM in ethanol, and was further diluted to 1 μM working solution using E3 medium. All embryos were treated with chemicals from 6 to 26 hpf.

Cell culture

Human umbilical vein endothelial cells (HUVECs) were cultured in EBM-2 medium (Lonza) as previously described (*5, 31*). Methyl-β-cyclodextrin (MβCD) was obtained

from Sigma (C4555) and prepared in serum-free EBM-2 medium. Mouse C166 endothelial cell (EC) line (ATCC, CRL-2581) were cultured in Dulbecco's Modified Eagle's Medium (DMEM), supplied with 10% fetal bovine serum (FBS).

Lentivirus infection

The C166 ECs were infected with the third generation lentiviral system following Addgene Lentiviral Guide. The plasmids: pRSV-Rev (Addgene, #12253), pMDLg/pRRE (Addgene, #12251), and pMD2.G (Addgene, #12259) were gifted from Dr. Didier Trono (*32*); pLJM1-EGFP (Addgene#19319) was from the Sabatini lab (*33*). After the cells were infected with nuclear Srebp2 overexpression virus for 96 hr, the supernatant was discarded and the selection medium was added (DMEM supplemented with 10% FBS and 5 μg/mL puromycin) to establish nuclear Srebp2 (nSrebp2) stable cell line.

HDL_3 isolation

We obtained fresh plasma of healthy donors from the blood bank at Houston Methodist Hospital. Kbr was added to the plasma and prepare a plasma density of 1.12 g/mL and subjected to ultracentrifugation at 35,000 rpm for 2 days at 4°C (ThermoFisher Sorvall WX 80). The fractions containing HDL were transferred to a new tube and used to prepare a KBr density of 1.21 g/mL. After an additional spin at 40,000 rpm for 3 days at 4°C, the HDL_3 fraction was collected and dialyzed against PBS with 2 mM EDTA. The purity of HDL_3 was validated by FPLC analysis and Coomassie Blue staining of SDS-PAGE-separated HDL_3. The HDL_3 preparation was assessed for possible endotoxin contamination using a LAL kit (ThermoFisher). The HDL_3 used for our cell culture assays contained endotoxin levels less than 50 pg/mg proteins, corresponding to 2.5 pg/mg in the cell culture media.

Quantitative RT-PCR

Quantitative RT-PCR (qRT-PCR) was performed as previously described (*34*). Briefly, RNA was isolated from zebrafish embryos using an RNeasy kit (Qiagen, 74104), and cDNA was reversely transcribed using the qScript cDNA supermix (Quanta Biosciences, Gaithersburg, MD). SYBR green-based (Genesee Scientific) qRT-PCR reactions were performed using the QuantStudio™ 12K Flex Real-Time PCR System (Invitrogen) according to the manufacturer's instructions, and biological triplicates were included for each sample. The mRNA expression levels of the investigated transcripts were normalized to that of *ef1a*. Primers used in qRT-PCR were: *ef1a* (GenBank Accession # NM_131263), *ef1a*-F (5'-ACCGGCCATCTGATCTACAA-3') and *ef1a*-R (5'-CAATGGTGATACCACGCTCA-3'); *srebf1* (GenBank Accession # NM_001105129.1), *srebf1*-F (5'-AGACTCTCTACAGCTCCTACAC-3') and *srebf1*-R (5'-CTGGATCGTCATTGGCTGAATA-3'); *srebf2* (GenBank Accession # NM_001089466.1), *srebf2*-F (5'-GATTCTGGAGACACAGGAAAC-3') and *srebf2*-R (5'-CTCTGGATAACACTGACAGACAC-3'). Mouse *Runx1* (GenBank Accession # NM_001111021.2), *Runx1*-F (5'-GGACATTCGGTCTTAGGGATTT-3') and *Runx1*-R (5'-CCTCAACATCTCATGCCTTCT-3'); mouse *Ef1a1* (GenBank Accession # NM_010106.2), *Ef1a1*-F(5'-GATCGATCGTCGTTCTGGTAAG-3') and *Ef1a1*-R(5'-AGTGGAGGGTAGTCAGAGAAG-3').

Whole-mount *in situ* hybridization (WISH)

WISH was performed as previously described (*35*). Briefly, embryos were fixed overnight with 4% paraformaldehyde (PFA) in phosphate buffered saline (PBS). Fixed embryos were rehydrated stepwise from methanol to PBS-0.1% Tween 20 (PBT) and subjected to proteinase K treatment. Afterwards, samples were washed in PBT and refixed at room temperature. After a wash with PBT, embryos were prehybridized at 70°C for 4 hr in the hybridization buffer (50% formamide, 5 × SSC, 500 μg/ml torula yeast tRNA, 50 μg/ml heparin, 0.1% Tween 20, 9 mM citric acid, pH 6.5), then hybridized overnight in hybridization buffer containing digoxigenin (DIG) labelled riboprobes. After hybridization, the experimental samples were washed sequentially at 70°C for 10 min, with each wash using the hybridization buffer 2 × SSC mixes (75%, 50%, 25%), followed by two washes with 0.2 × SSC for 30 min at 70°C. Additional sequential washes were performed at room temperature with 0.2 × SSC in PBT (75%, 50%, 25%). Samples were then incubated in PBT with 2% heat-inactivated goat serum and 2 mg/ml bovine serum albumin (blocking solution) for 4 hr and then incubated overnight at 4°C in blocking solution containing diluted DIG-antibodies (1:5,000) conjugated with alkaline phosphatase (AP) (Roche). To visualize WISH signals, samples were washed in AP reaction buffer (100 mM Tris-HCl, pH 9.5, 50 mM $MgCl_2$, 100 mM NaCl, 0.1% Tween 20) and then incubated with the AP reaction buffer that contains NBT/BCIP substrate (Promega) for appropriate time. The reaction was stopped using Stop buffer (1 × PBS pH 2.2, 1 mM EDTA, 0.1% Tween 20) when a proper signal was visualized under a dissection microscope.

Western blot

Zebrafish or HUVECs were lysed on ice with the lysis buffer (50 mM Tris-HCl, pH 7.5, 4 mM sodium deoxycholate, 1% Triton X-100, 150 mM NaCl, 1 mM EDTA and a protease inhibitor cocktail from Sigma). Western blotting was performed as previously described (*36*). Briefly, protein concentration was determined with a Pierce BCA Protein Assay Kit (Thermo Scientific) and an equal amount of proteins were separated on 4-15% a Mini-PROTEAN TGX Precast Protein Gel (Bio-rad). The proteins in gel were then transferred to Immobilon-P Membrane (Millipore), which was blocked with 5% non-fat milk dissolved in 0.05% Tween-20 in TBS (TBST) for 1 hr at room temperature, and then was incubated with the corresponding primary antibody overnight at 4 °C. After three washes with TBST, the membranes were further incubated with a HRP-conjugated secondary antibody for 1 hr at room temperature. The blot was developed using the Amersham ECL Prime Western Blotting Detection Reagent (GE Healthcare, #RPN2232). The antibodies used were: Guinea Pig anti-Aibp2 (*5*), mouse anti-Srebp2 (Novus, #NBP1-54446), mouse anti-LAMIN A/C (Cell Signaling, #4777S), rabbit anti-β-Tubulin (Cell Signaling, #2148S), goat anti-Guinea Pig HRP-conjugated antibody (Jackson Labs, #106-035-003), goat anti-mouse HRP-conjugated antibody (Jackson Labs, #115-035-003), and goat anti-rabbit HRP-conjugated antibody (Jackson Labs, #111-035-144).

Free cholesterol measurement

Free cholesterol content in zebrafish was measured using a colorimetric assay (BioVision) as previously described (*5*). Sixty embryos were pooled for each sample measurement. Total cholesterol content in mouse plasma was measured in the Mouse

Metabolism Core at Baylor College of Medicine.

Fluorescence Activated Cell Sorting (FACS) analysis of HSPCs in zebrafish
FACS analysis was performed using *Tg(cmyb:GFP; kdrl:mCherry)* HSPC reporter zebrafish as previously described (*37, 38*). Briefly, one-cell stage *Tg(cmyb:GFP; kdrl:mCherry)* embryos were injected with 1 nl of control (0.2 mM), *apoa1bp2* (0.1 mM), or *srebf2* (0.2 mM) MOs and collected at 48 hpf. Approximately 50 embryos per group were dissociated, resuspended in 1 × DPBS with 2% heat-inactivated FBS, and analyzed by BD LSR II flow cytometer in the presence of SYTOX Red Dead Cell stain (5 nM; Life Technologies). Data were analyzed using FlowJo software.

Confocal microscopy
Anaesthetized zebrafish embryos (treated at 10 hpf with 0.003% 1-phenyl 2-thiourea) were housed in a sealed chamber (Invitrogen) in a small drop of 0.02% tricaine (Sigma) containing E3 medium and imaged using a Olympus FluoView FV1000 confocal microscope. Z-stacks were acquired with a 3-μm step, and max-projection confocal images analyzed using ImageJ software (NIH). All three-dimensional reconstructions were performed with the same threshold settings.

Srebp2 binding site prediction
The Srebp2 binding sites on *notch1b* and *ldlr* promoters were predicted using Jaspar (http://jaspar.genereg.net/cgi-bin/jaspar_db.pl).

Chromatin immunoprecipitation (ChIP)
The ChIP assays were performed as previously described (*35*). Briefly, *Tg(kdrl:Gal4ER^{T2}; UAS:Flag-nSrebp2-2A-mCerulean3)* embryos were treated with 5 μM 4OHT or an equal amount of ethanol at 6 hpf, AGM regions were isolated from the 26 hpf embryos, and cross-linked in 2.2% PFA. After termination of crosslink using 0.125 M glycine and subsequent PBS washing, the nuclei were disrupted in lysis buffer (50 mM Tris-HCl [pH 8.0], 10 mM EDTA, 1% SDS, protease inhibitors, and phosphatase inhibitors). The nuclear extracts were then sonicated to generate chromatin DNA fragment (300-600 bp). Following removal of cell debris, 5% of the sample was kept as input and the rest in IP dilution buffer (16.7 mM Tris-HCl [pH 8.0], 167 mM NaCl, 1.2 mM EDTA, 1.1% Triton X-100, and 0.01% SDS, protease inhibitors). Sample extracts were pre-cleared for 2 hr at 4 °C using 2 μg sheared salmon sperm DNA (Life Technologies) and 45 μl of protein A Sepharose (50% slurry in dilution buffer) (Sigma). Immunoprecipitations were carried out overnight at 4 °C with an anti-Flag antibody (Sigma, F3165). Immune complexes were captured with protein A Sepharose and washed three times with low salt buffer (20 mM Tris-HCl [pH 8.0], 0.1% SDS, 1% Triton, 2 mM EDTA, 200 mM NaCl) and additional three times with TE. The immune complexes were then eluted with 1% SDS (v/v), 0.1 M $NaHCO_3$, and heated overnight at 65°C to reverse the cross-link. After proteinase K digestion (100 μg/ml, 1 hr at 50°C), DNA fragments were purified on QIAquick Spin columns (Qiagen) in 50 μl elution buffer and 1 μl was used for each qPCR reaction. Primer sequences are listed below. Data were presented as enrichment of the precipitated target sequences, as compared to the input DNA.

Primers used for ChIP-qPCR

Gene	Primer Sequences (5' - 3')
Zebrafish	
notch1b	site1-F: CAGTCATCAGAAGCATGCGA
	site1-R: ACTTTAGATGTGTGCGCTCTG
	site2-F: AGCATTCATTGCAGCTCATTC
	site2-R: CACGCCCTCCCTTTAAACT
	nonbinding-F: GGGTTGACTTATGGCAGGTATTA
	nonbinding-R: CGTCCCAAATGGAGCACTAA
ldlr	F: GATAAGCCGAGTAGCTGAAAGT
	R: GGGATTCGGTGGTGTGATTTA
Mouse	
Notch1	F: CGG GCT CGT TCC TTC AC
	R: AGA GCC TCA CTA GTG CCT
	nonbinding-F: CAA AGG CTC TGA GGC AGA A
	nonbinding-R: GTG AGC AGG CTC TGG AAA T
Ldlr	F: CGC TCA GTG AGG TGA AGA TT
	R: GCA CGC CCA GAG TCA TT
	nonbinding-F: GCA GAG GCA GGT GGA TTT
	nonbinding-R: TCT AGC CCA TCT TTG GTT GAT T
Hmgcr	F: GCC GCC AAT AAG GAA GGA T
	R: CAG TGG GCG GTT GTT AGG
	nonbinding-F: CAT CCT GGG TCC TAC ATG AAA C
	nonbinding-R: GAT TAA CCA CAG GAG TGA TCC G
Srebf2	F: GAG TCC CGC TAT GCA AAT CT
	R: CCC AAG TTT GTT GTC AAT GGG
	nonbinding-F: CCT TGA TAG CGA TCG AGT TAC C
	nonbinding-R: GCA AAG CCA AGT AAG GAA GAT G

High cholesterol diet feeding of zebrafish and Western diet feeding of mice

Tg(cmyb:EGFP; kdrl:mCherry) double transgenic fish were fed either control diet or the same diet supplemented with 4 % w/w cholesterol (HCD) for one month, as previously described (*39*). Eight weeks old *Ldlr*$^{-/-}$ mice were fed control diet, Western diet (WD, 42% fat and 0.2% cholesterol from Envigo, Cat No. TD88137), or betulin diet (WD supplemented with 600 ppm betulin) for 16 weeks.

Murine AGM and bone marrow isolation and FACS analysis

Embryos from timed pregnant female *Ldlr*$^{-/-}$ mice were micro-dissected for isolation of E11.5 AGM regions as previously described (*40, 41*). Tissues were dissociated by treatment with 0.25% collagenase at 37 °C for 30 min and filtered through a 70-μm cell strainer. Cells were immunostained with the following antibodies and used for FACS analysis after proper wash with DPBS plus 2% FBS. Antibody information: biotin mouse anti-Rat IgG2a (Cat No. BDB553894), rat anti-mouse CD144 (Cat No. BDB555289), anti-mouse CD117 (c-Kit) APC (Cat No. 50-112-9173), mouse anti-mouse CD45.2 PE-Cy7 (Cat No. BDB560696) and PE-streptavidin (Cat No. BDB554061).

Bone marrow was collected for the analysis of HSPCs 16 weeks after feeding WD or WD with betulin, as previously described (*42*). In brief, bone marrow was flushed from the tibia and femur bones with DPBS plus 2% FBS, dissociated to single cell suspension, and filtered through a 70 μm cell strainer. The resulting single cell suspension was subjected to RBC lysis (Cat No. 555899) and incubation with the following antibodies from Biolegend: Pacific Blue anti-mouse Lineage Cocktail (Cat No. 133310), PerCP/Cy5.5 anti-mouse Ly-6A/E (Sca-1) antibody (Cat No. 108124) and APC/Cy7 anti-mouse CD117 (c-kit) (Cat No. 105826). The immunostained cells were analyzed using a five-laser BD LSR II flow cytometer.

RUNX1 immunostaining

The E11.5 embryos from pregnant female C57BL/6J (JAX, Stock No: 000664) mice were micro-dissected for isolation of AGM regions as above described. The c-Kit^{+}CD144^{+}CD45.2^{-} cells were collected and specimens were prepared using cytospin. Specimens were fixed in 4% PFA for 20 min, and then permeabilized in 0.3% Triton X-100 in PBS for 10 min. After blocking with 5% BSA in PBS for 1 hr at room temperature, the specimens were immunostained with anti-RUNX1 antibody (Santa Cruz Biotechnology, Cat. No. sc-365644) in blocking buffer at 4 °C overnight. After proper wash, the specimens were incubated with Alexa Fluor 594-conjugated secondary antibodies for 1 hr at room temperature, and then with DAPI for 5 min following PBS wash. After mounting in anti-fade mounting medium, the images were captured using Olympus FV 1000 confocal microscope.

Bromodeoxyuridine (BrdU) incorporation and immunostaining

BrdU incorporation assays were carried out as previously described (*43*). In brief, *Tg(cmyb:GFP)* embryos were incubated with 10 mM BrdU on ice for 30 min and incubated with E3 medium in the 28ºC incubator for an additional 2 hr. Embryos were then fixed in 4% PFA at 30 or 36 hpf. Subsequently, the embryos were dehydrated with methanol and stored at -20ºC overnight. After rehydration, the embryos were treated with 10 μg/ml Proteinase K for 30 min and re-fixed in 4% PFA for 30 min. After blocking with blocking buffer (1% BSA, 10% normal goat serum, 0.3% Triton-X100 and 1% DMSO in PBST) for 2 hr at room temperature. The embryos were stained with anti-GFP primary antibody (Invitrogen) and corresponding Alexa Fluor 488-conjugated secondary antibodies (Invitrogen). The embryos were further treated with 2N HCl for 1 hr at room temperature, and immunostained with mouse anti-BrdU primary antibody (Roche) and proper Alexa Fluor 594 secondary antibody (Invitrogen). Images were captured using Olympus FV 1000 confocal microscope.

Assay for Transposase-Accessible Chromatin sequencing (ATAC-seq)
The ATAC-Seq was performed using 50,000 c-Kit^{+}CD144^{+} CD45.2^{-} cells isolated from AGM region of E11.5 wild-type B6 mouse embryos. The Tn5 transposome was purified and assembled following a published protocol (*44*). The permeabilization was performed with 50 µl cold ATAC-RSB buffer (0.1% NP40, 0.1% Tween-20, and 0.01% Digitonin) and the transposition was performed with 50 µl transposition mix (10 µl 5× HEPES DMF Buffer, 3 µl 5 µM Tn5 transposome, 37 µl PBS, 0.5 µl 10% Tween-20, and 0.5 µl 1% digitonin) and incubated at 37° for 30 min. After transposition, the cleaned-up DNA fragments were pre-amplified for 5 cycles using NEB Q5 master mix. Each reaction contains 2.5 µl of 25 µM i5 primer, 2.5 µl of 25 µM i7 primer, 25 µl 2× NEB Q5 master mix, and 20 µl cleaned up samples. PCR settings were 5 min at 72°C, 30 sec at 98°C, and followed by additional 5 cycles (98°C for 10 sec, 63°C for 30 sec, 72°C for 1 min). After pre-amplification, 1 µl of the pre-amplified mixture was used to run a 10 µl qPCR test to determine the optimal amplification cycle. The final amplified DNA library was purified using Qiagen DNA purification kit and sequenced on NextSeq 500 with SE75 strategy.

Volunteer recruitment
Two hundred Chinese male subjects (age 45.00±10.57 years) were recruited for this study at the Outpatient Center, Department of Geriatric Medicine of Xiangya Hospital, Central South University between February and May 2017. All subjects underwent comprehensive physical examinations and routine biochemical analyses of peripheral blood (table S4). Exclusion factors included diseases affecting the metabolic state or not suitable to participate in this study, which includes hyperthyroidism, hypothyroidism, cancer, or other disorders affecting the functions of heart, liver, or kidney, etc. The study was approved by the human research ethics committee of Xiangya Hospital at the Central South University, and informed consents were obtained from all subjects.

Human blood collection and analysis
Five ml of intravenous blood samples from the healthy individuals were collected after 12 hr of overnight fasting. Plasma was separated and stored at -80°C. Plasma LDL-C was determined by enzymatic methods using a Hitachi 7600 analyzer. The CD34^{+}CD45^{+} HSPC population of the blood samples were immunostained and determined by FACS according to the International Society of Hematotherapy and Graft Engineering (ISHAGE) guidelines (*45*).

Position-wise cumulative analysis of Srebp2 binding motif or Srebp2 ChIP-Seq peak enrichment relative to TSS
To determine the enrichment levels of Srebp2 binding motif (Fig. 4C) or binding sites (Fig. S18C) near individual TSS groups, we developed CAGRE, a new bioinformatics tool for Cumulative Analysis of Genomic Region Enrichment. CAGRE can be downloaded at https://github.com/jielv/CAGRE and adopted for the analysis of other transcription factors.

Statistical analysis for Fig. S20D

The statistical analysis was performed using SPSS 21.0 (Chicago, Illinois, USA). Data were expressed as mean±SD. Mann-Whitney U test was applied for comparison between the low LDL-C and high LDL-C groups. Spearman's correlations were used to examine the association of plasma LDL-C and other parameters, and $p < 0.05$ was considered statistically significant.

Data Analysis

ChIP-seq and ATAC-seq analyses

We used Bowtie v1.1.0 to map sequencing reads to the mouse reference genome version mm9, requiring single best match for each read across the genome. We used the Dpeak function in DANPOS v2.2.3 to calculate reads density as the number of mapped reads covering each base pair (bp) of the genome and to define enriched peaks with read density cutoff being Poisson test P value 1e-8. For each dataset, we normalized the total number of mapped reads to 25 million and extended each read at the 3' end to be 200 bp long. The function Dpeak in DANPOS v2.2.3 also accounts for variations between biological replicates of the same ChIP/ATAC experiment. We set the bin size to 10 bp, and set the smooth width to 0 bp so that there was no additional smoothing step in the calculation of reads density. Input effect was subtracted from the ChIP-Seq data by DANPOS v2.2.3. For reference gene set, we downloaded the KnownGene provided at the Table Browser page of UCSC Genome Browser (http://genome.ucsc.edu/cgi-bin/hgTables). We used the function Profile in DANPOS v2.2.3 to plot average reads density around transcription start sites (TSS) or gene body and generated data matrices for heat maps of ChIP-Seq reads density around each TSS. To map peaks to individual genes, we used the function Selector in DANPOS v2.2.3 to retrieve peaks that were located within the region from -5 kb to +5 kb with respect to TSS.

RNA-Seq analysis

For RNA-seq data, we used TopHat v2.0.12 to map the raw reads in FASTQ format to the mm9 mouse reference genome with the following parameters settings: --mate-std-dev 200 -p 8 -r 200. The mapped reads for each sample were saved in a BAM format file and we used UCSC KnownGenes as reference genes. The BAM file and reference genes were subjected to the Cuffdiff function in Cufflink suite v2.2.1 to calculate read counts and gene expression (fragments per kilobases per million, or FPKM). To identify differentially expressed genes based on read counts between different RNA-Seq samples, we used the normalizeQuantiles, estimateCommonDisp and estimateTagwiseDisp functions in the R package edgeR v3.14.0 to normalize the read counts, estimate common dispersion, and estimate moderated tag-wise dispersion, respectively. The edgeR then defined differential genes based on a negative binomial test. In the final list of differential genes, we required each differential gene to have a differential FDR value smaller than 0.05 and FPKM value larger than 1 in at least one sample. We used the tool MultiExperimet Viewer (MEV v10.2) to plot the heat maps of relative expression levels for differentially expressed genes between ECs and HECs or between HECs and HSCs.

Function enrichment analysis

We used DAVID v6.7 (https://david.ncifcrf.gov) for Gene Ontology and KEGG pathway analysis. Gene Ontology Biological processes or KEGG pathways with p values smaller than 0.05 were defined as significantly enriched.

Motif analysis

We used HOMER v4.10 to detect known Srebp2 binding motif instances around gene promoters and to infer de novo Srebp2 binding motif from Srebp2 ChIP-Seq data (*17*). For known Srebp2 motif instance detection, we downloaded the position weight matrices (PWM) from the JASPAR 2018 core database. We scanned the Srebp2 PWD using annotatePeaks.pl program of HOMER to find instances of motifs near Srebp2 ChIP-Seq peaks. Motif density profile across Srebp2 peaks with positive hits was generated using the "-hist" parameters of annotatePeaks.pl program and homemade python script. We used findMotifsGenome.pl program of HOMER to infer de novo Srebp2 binding motif using 400 bp regions around the center of Srebp2 binding peaks.

Experimental design and statistical analysis

All animal experiments were performed using randomly assigned embryos without the investigator's blinding. Sample sizes were chosen after estimating effect size, and data were analyzed for statistical significance after at least three independent repeats. All the data were representative of three independent experiments using three different clutches of embryos and were expressed as Mean±SE. Statistical differences were analyzed using unpaired two-tailed Student's t-tests unless otherwise specified, with $p < 0.05$ considered as statistically significant. $*$ $p < 0.05$; $**$ $p < 0.01$; $***p < 0.001$; $****p < 0.0001$; NS, not significant.

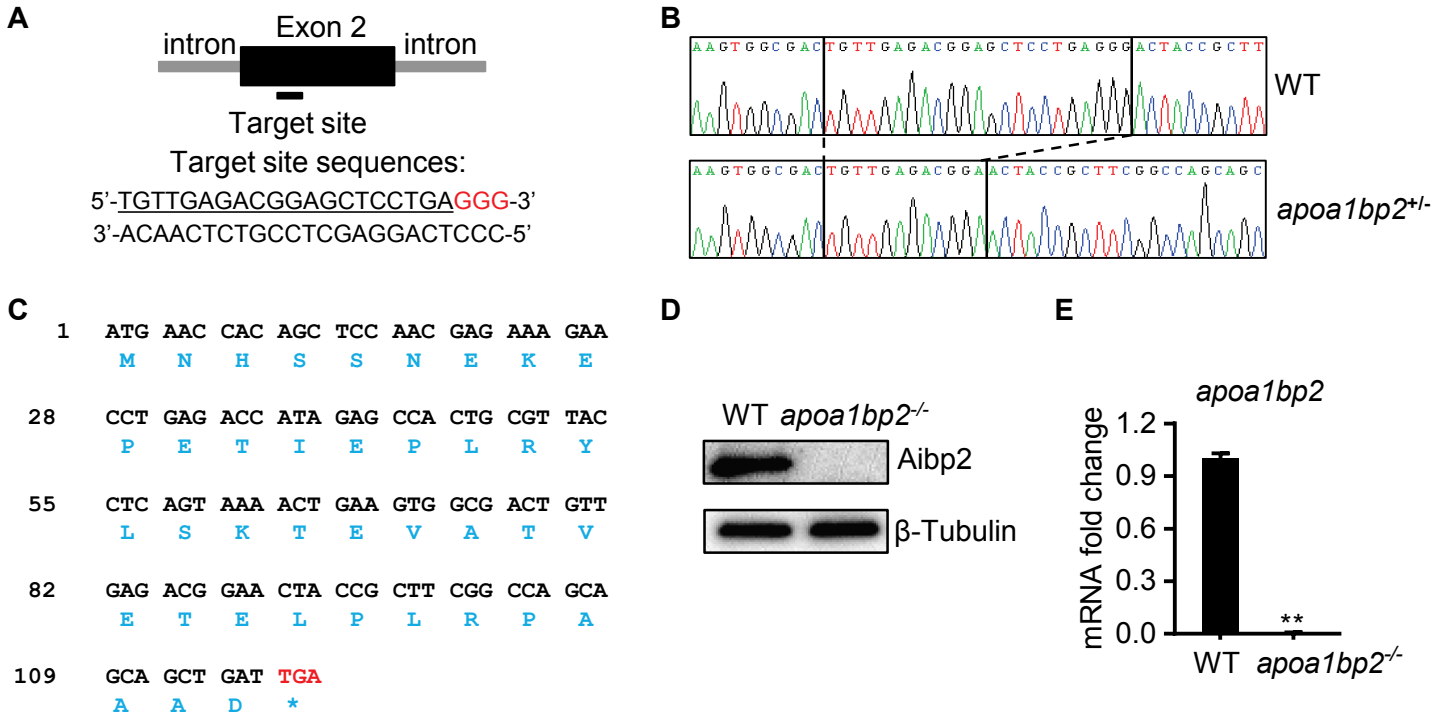

Fig. S1. Generation of Aibp2 knockout zebrafish. Diagram showing position of the target site and its sequence (underline) in zebrafish *apoa1bp2* locus. PAM sequence (GGG) is shown in red. **B.** Sanger sequencing result of heterozygous mutants revealed an 11-bp genomic DNA fragment deletion from the target site. The PCR amplicons that span the mutated *apoa1bp2* region were ligated into a T-vector and subsequently transformed into competent cells. Single positive colonies were selected for sequencing. **C.** The 11-bp deletion resulted in a presumptive stop codon (red) in Exon2 of *apoa1bp2*. **D** and **E**. Western blot and qRT-PCR analyses of pooled 26 hpf zebrafish (n=20) show the absence of Aibp2 (**D**) and *apoa1bp2* mRNA (**E**).

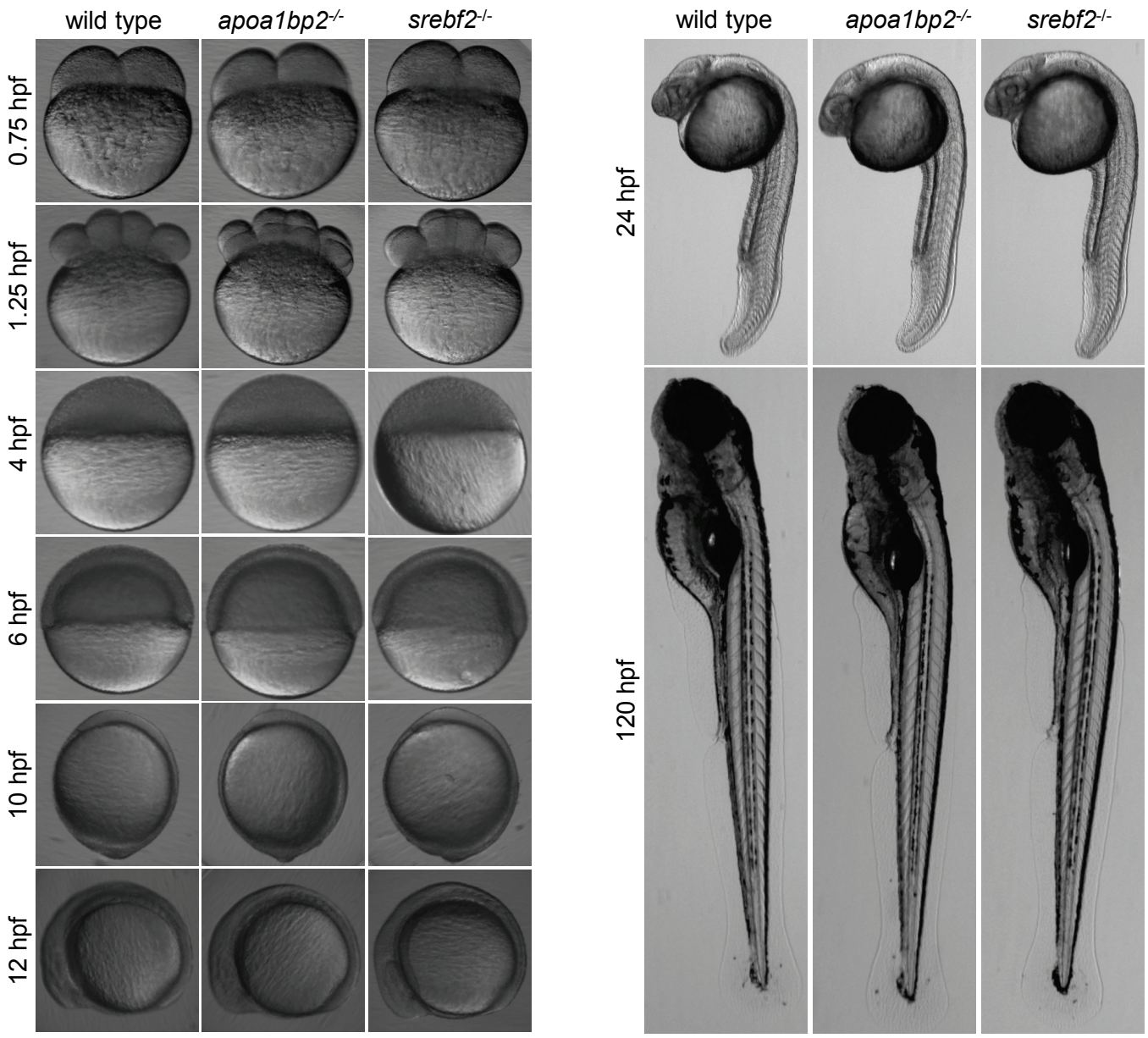

Fig. S2. No gross phenotypic defect observed in Aibp2 and Srebp2 knockout zebrafish. Zebrafish embryos at the indicated developmental stages were collected and images of live zebrafish embryos captured. hpf: hour(s) post fertilization.

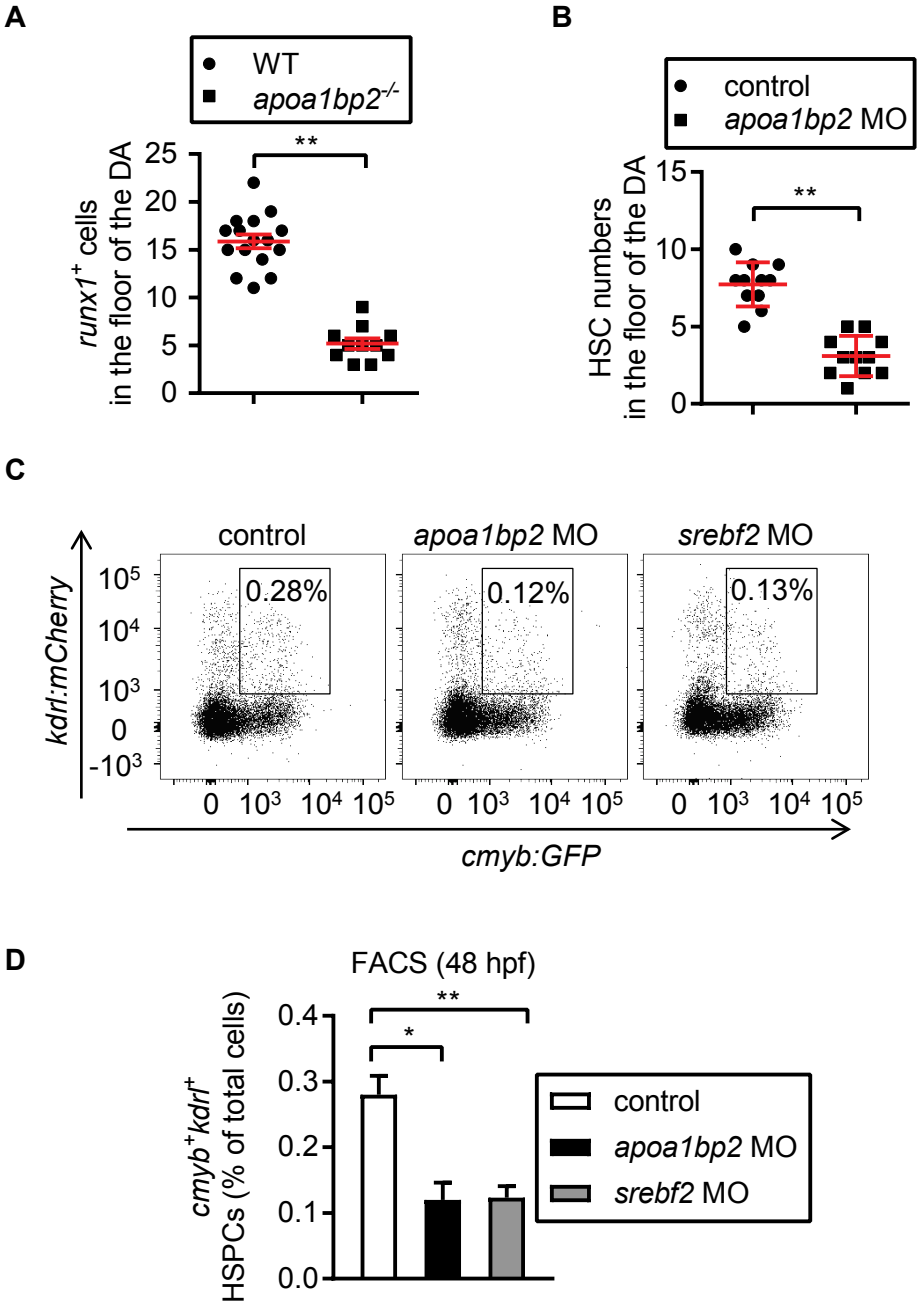

Fig. S3. Loss of Aibp2 impedes hematopoiesis. A. Quantification of *runx1*$^{+}$ HSCs in the floor of DA in **Fig. 1A**. **B.** Quantification of *cmyb*$^{+}$*kdrl*$^{+}$ HSCs in **Fig 1B**. The whole animals of 48 hpf *cmyb:GFP; kdrl:mCherry* zebrafish was homogenized and *cmyb*$^{+}$*kdrl*$^{+}$ HSCs were analyzed using FACS (**C**) and quantified (**D**) in control, Aibp2, or Srebp2 knockdown animals . Mean±SE; *p<0.05; **p<0.01.

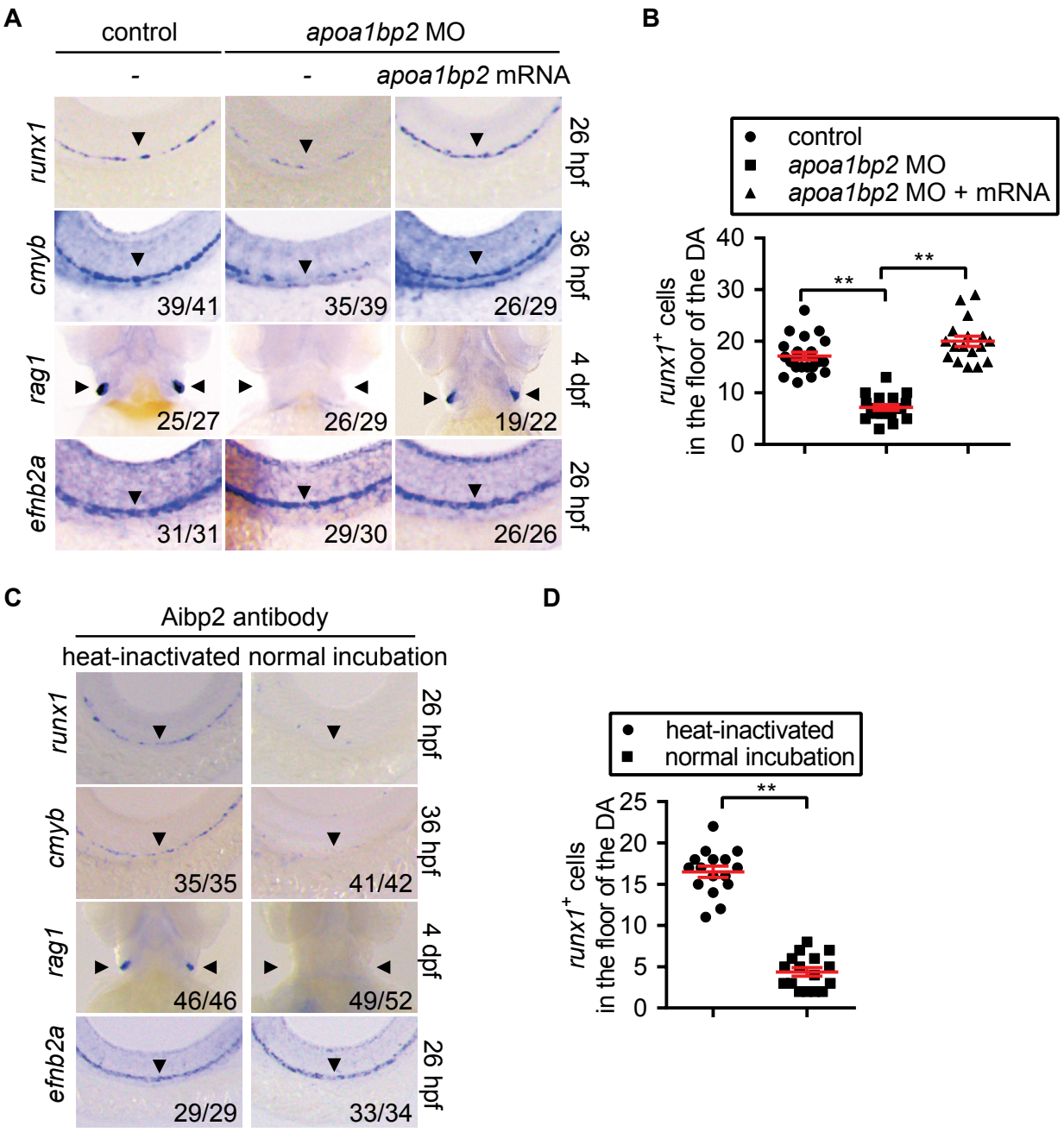

Fig. S4. Aibp2 deficiency impairs HSPC emergence. A. WISH analysis of *runx1*, *cmyb*, *rag1,* and *efnb2a* expression in control MO-injected (control), *apoa1bp2* MO-injected or a combination of *apoa1bp2* MO and *apoa1bp2* mRNA-injected embryos at the indicated time on the right. Arrowheads denote DA or thymus. **B.** Quantification of *runx1*$^{+}$ HSCs in panel **A**. **C**. Expression of *runx1*, *cmyb*, *rag1*, and *efnb2a* in control (heat-inactivated) or Aibp2 antibody-injected animals. Arrowheads indicate the location of DA or thymus. **D**. Quantification of *runx1*$^{+}$ HSCs in panel **C**. Mean±SE; **p<0.01.

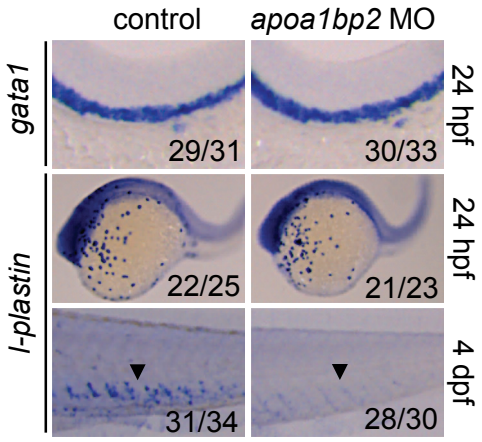

Fig. S5. Aibp2 knockdown has no effect on primitive hematopoiesis. WISH analysis of *gata1* and *l-plastin* in the control or *apoa1bp2* morphants. Arrowheads indicate *l-plastin*$^{+}$ leukocytes derived from definitive hematopoiesis.

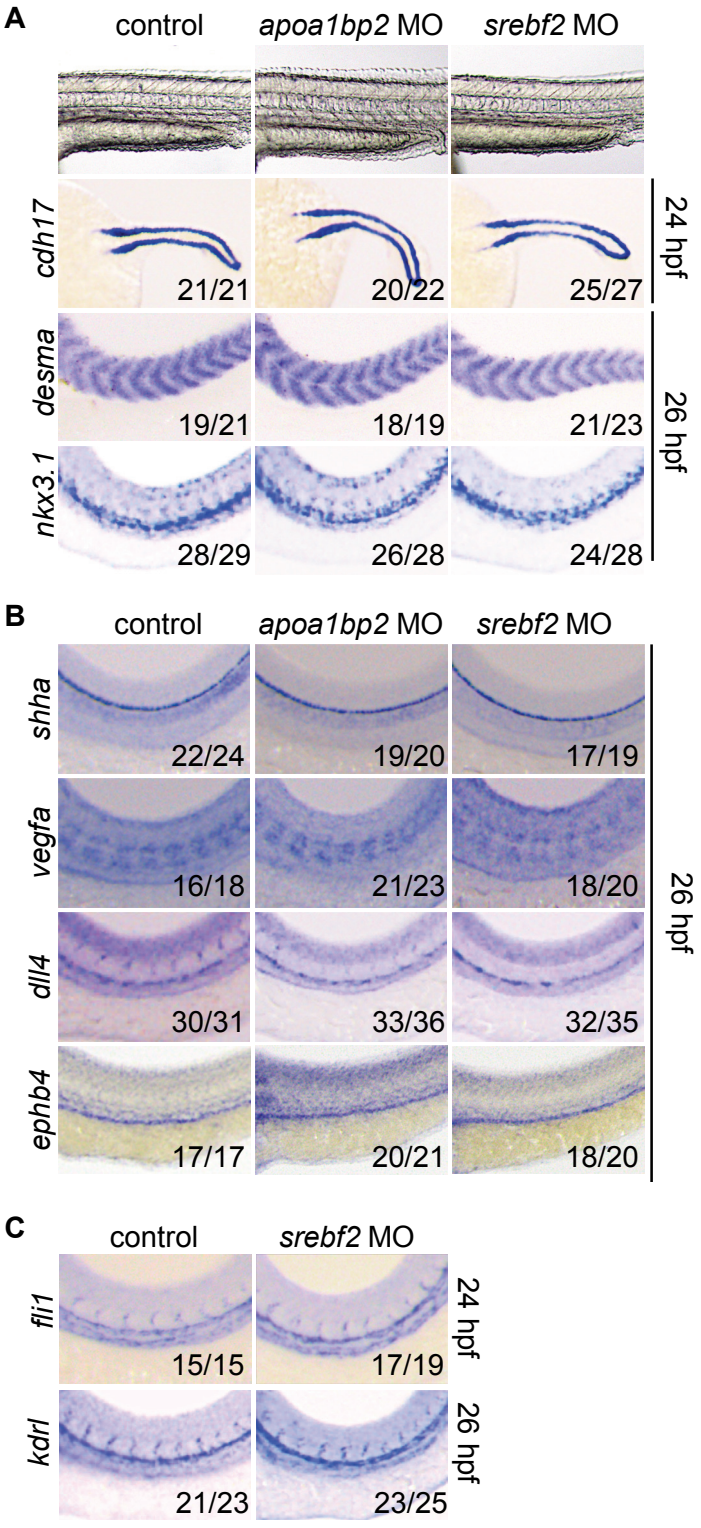

Fig. S6. Normal arterial specification and muscle development in *apoa1bp2* or *srebf2* morphants. A. Bright field image and expression of *cdh17* (a pronephros marker), *desma* (a somite marker), and *nkx3.1* (a sclerotome marker) in control, *apoa1bp2, or srebf2* morphants. **B.** WISH analyses of *shha* and *vegfa* (two shh pathway genes), *dll4 (*an arterial gene), and *ephb4* (a venous gene) in control, *apoa1bp2,* or *srebf2* morphants. **C.** The expression of *fli1* and *kdrl* (two pan-endothelial genes) in control or Srebp2-deficient animals.

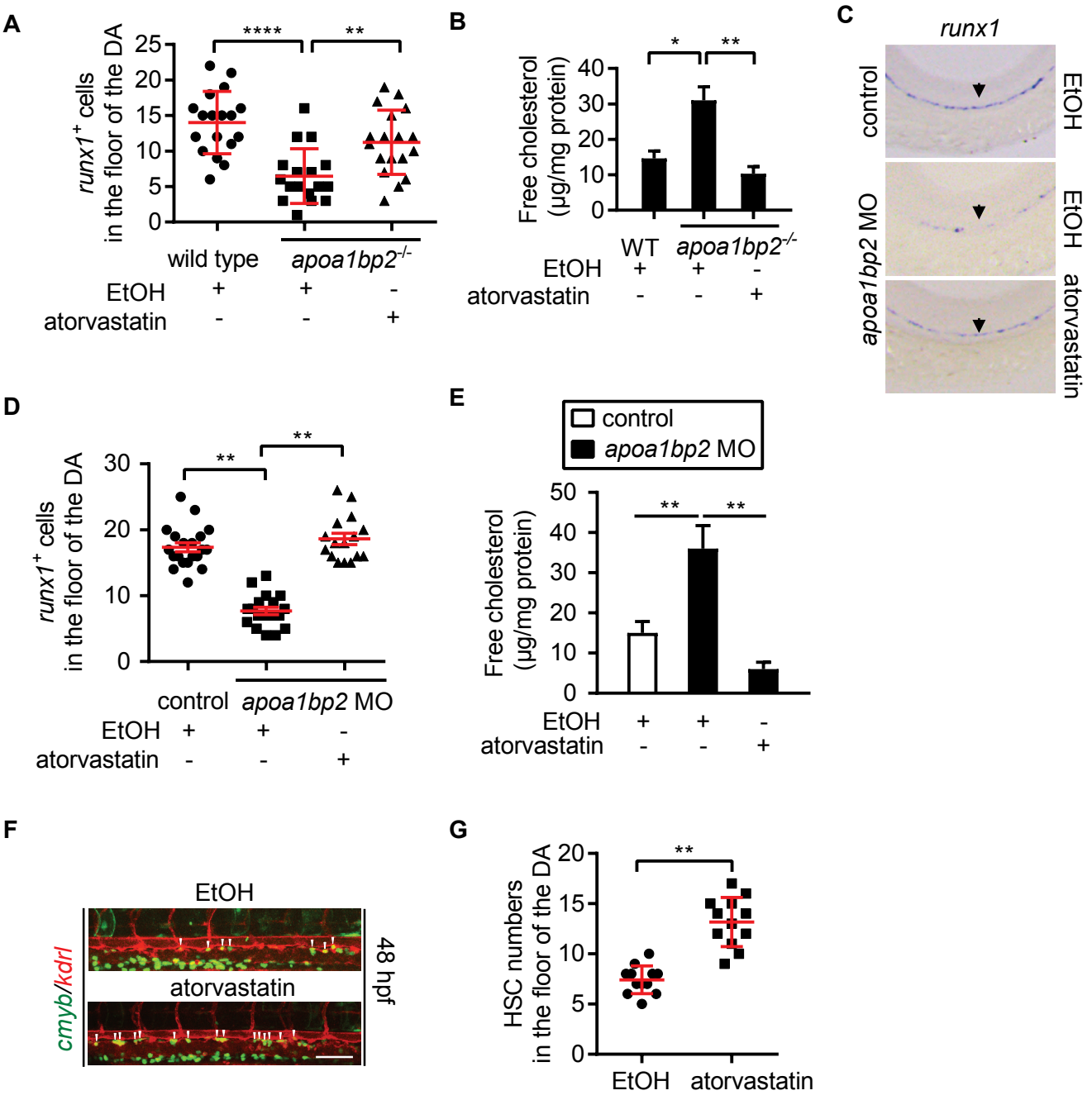

Fig. S7. Statin effect on hematopoiesis. A. Quantification of *runx1*$^{+}$ HSCs in **Fig. 1C**. **B.** Free cholesterol measurements in control or Aibp2 knockout zebrafish treated with vehicle (ethanol; EtOH) or atorvastatin (1 μM). **C**. The expression of *runx1* in control or *apoa1bp2* morphants treated with vehicle (EtOH) or atorvastatin (1 μM). Arrowheads indicate DA. **D**. Quantification of *runx1*$^{+}$ HSCs in the floor of DA of panel **C**. **E.** Free cholesterol measurements in the indicated embryos. **F.** Confocal imaging of HSC emergence in the transgenic *cmyb:GFP; kdrl:mCherry* zebrafish. **G**. Quantification of *cmyb*$^{+}$*kdrl*$^{+}$ HSCs in panel **F**. Scale bar: 100 μm. Mean±SE; *p<0.05; **p<0.01; ****p<0.0001.

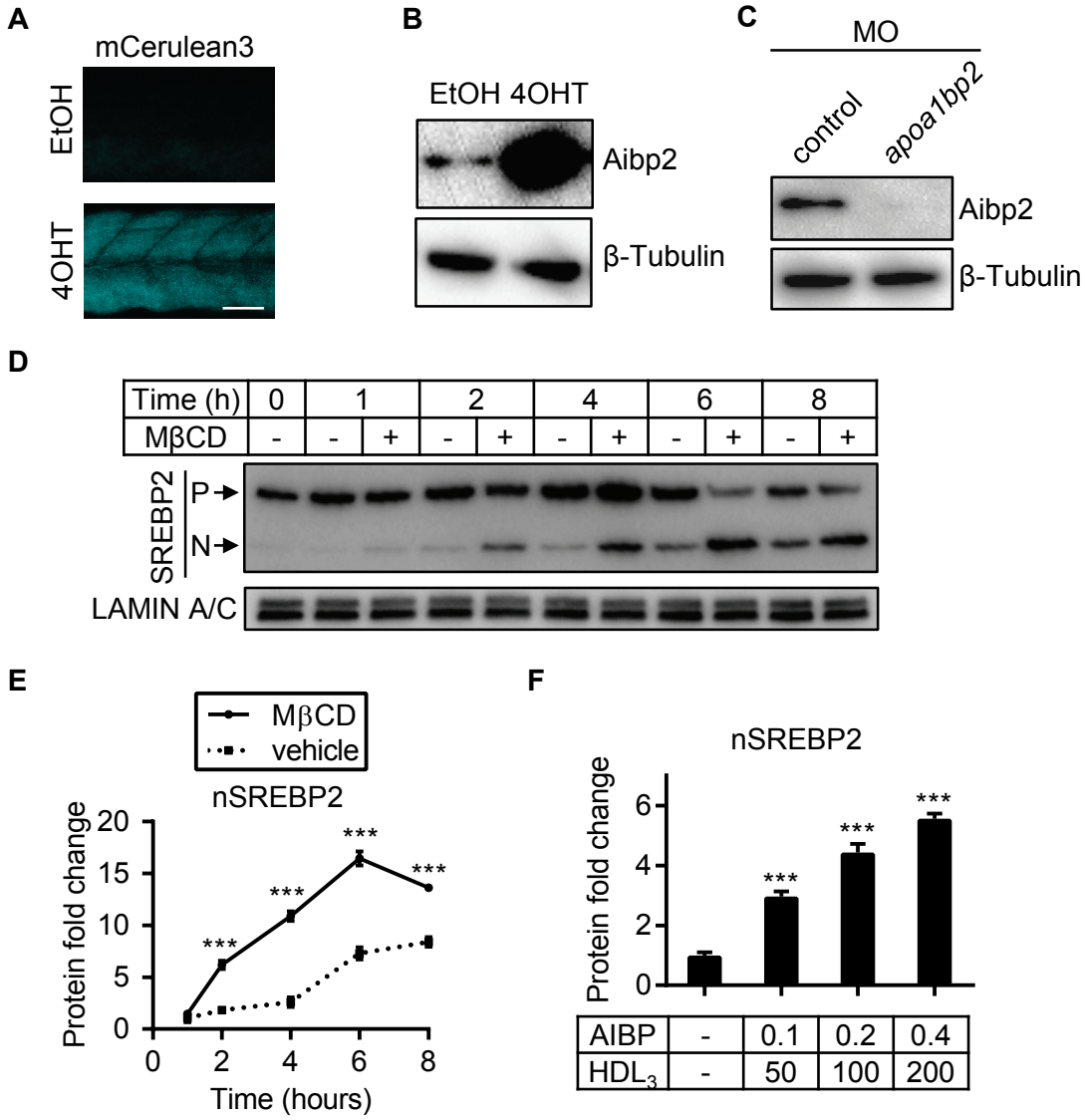

Fig. S8. AIBP activates Srepb2. A. 4OHT-induced Aibp2-2A-mCerulean3 expression in *hsp70:Gal4ER^{T2}; UAS:apoa1bp2-2A-mCerulean3* transgenic zebrafish. **B.** Immunoblots of Aibp2 expression in embryos from panel **A**. **C.** Immunoblotting of Aibp2 and β-Tubulin in control and *apoa1bp2* morphants. **D.** Immunoblots of SREBP2 in HUVECs pre-treated with MβCD or control media for 30 min, and then switch to serum-free EBM-2 medium for the indicated time. P, precursor form; N, nuclear form. **E.** Protein fold change of the transcriptionally active nuclear SREBP2 (nSREBP2) in panel **D**. **F.** Protein fold change of nSREBP2 in **Fig. 2D**. Statistical difference was measured using two-way ANOVA (**E**) and one-way ANOVA (**F**). Mean±SE; ***p<0.001. Scale bar: 100 μm.

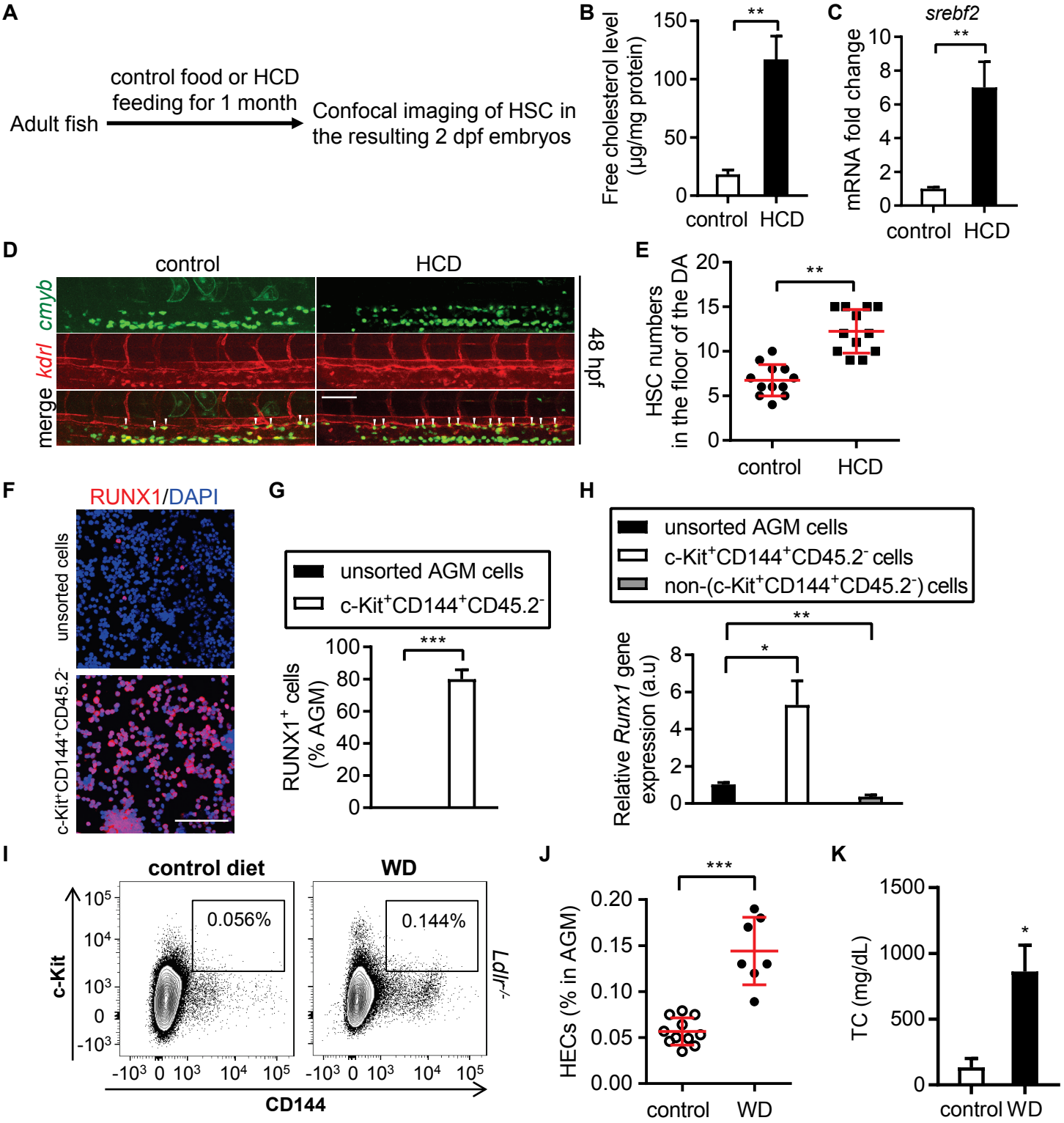

Fig. S9. Hypercholesterolemia augments HSC emergence. A. Experimental design. **B.** Free cholesterol measurements in the embryos produced from control or HCD-fed female zebrafish. **C.** Quantitative RT-PCR analysis of *srebf2* transcripts. **D.** Embryos produced from control or HCD-fed female zebrafish were imaged at 48 hpf by confocal microscope. Arrowheads show *cmyb*$^{+}$*kdrl*$^{+}$ HSCs in the floor of DA. **E.** Quantitative *cmyb*$^{+}$*kdrl*$^{+}$ cells in panel **D**. **F.** Confocal imaging of RUNX-1 antibody-stained unsorted AGM cells and HECs, which may contain a minor portion of hematopoietic precursors. **G.** Quantitative data of RUNX1^{+} cells (%) in the c-Kit^{+}CD144^{+}CD45.2^{-} cells and unsorted cells isolated from the AGM region. **H.** Quantitative RT-PCR analysis of relative *Runx1* gene expression in the indicated cell populations. The *Runx1* gene expression value was first normalized to that of *Ef1α* mRNA levels and then further normalized to the value of unsorted AGM cells. **I.** FACS analysis of HECs (c-Kit^{+}CD144^{+}CD45.2^{-}). Eight week-old female LDLR knockout mice were fed with control or Western diet (WD) for 8 weeks, then E11.5 embryonic mice were obtained from these hypercholesterolemic females, and AGM dissected for FACS analysis. **J.** Quantification of HECs in embryos produced from control or WD-fed female mice. **K.** Total plasma cholesterol (TC) measurements. Mean±SE; *p<0.05; **p<0.01; ***p<0.001. Scale bar: 100 μm.

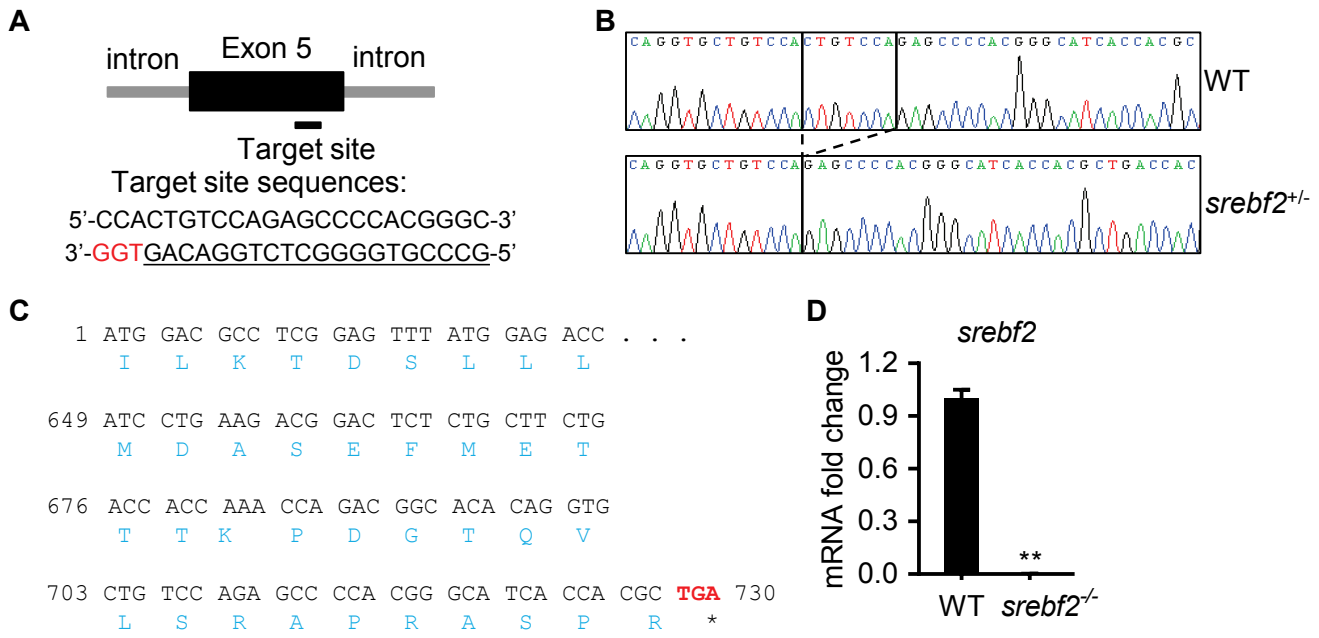

Fig. S10. Generation of Srebp2 knockout zebrafish.
A. Diagram showing position of the target site and its sequence (underline) in zebrafish *srebf2* gene locus. TGG (red) is the PAM sequence. **B.** Sanger sequencing result of a heterozygous mutant detected a 7-bp genomic DNA fragment deletion from the target site. Individual positive colonies containing the PCR amplicons that span the mutated *srebf2* region (in a T vector) were prepared and sent to DNA sequencing. **C.** The 7-bp deletion resulted in a new stop codon (red) that appeared in Exon 5 of *srebf2*. **D.** Quantitative PCR analysis of *srebf2* expression in WT and Srebp2 knockout zebrafish. Mean±SE; **p<0.01.

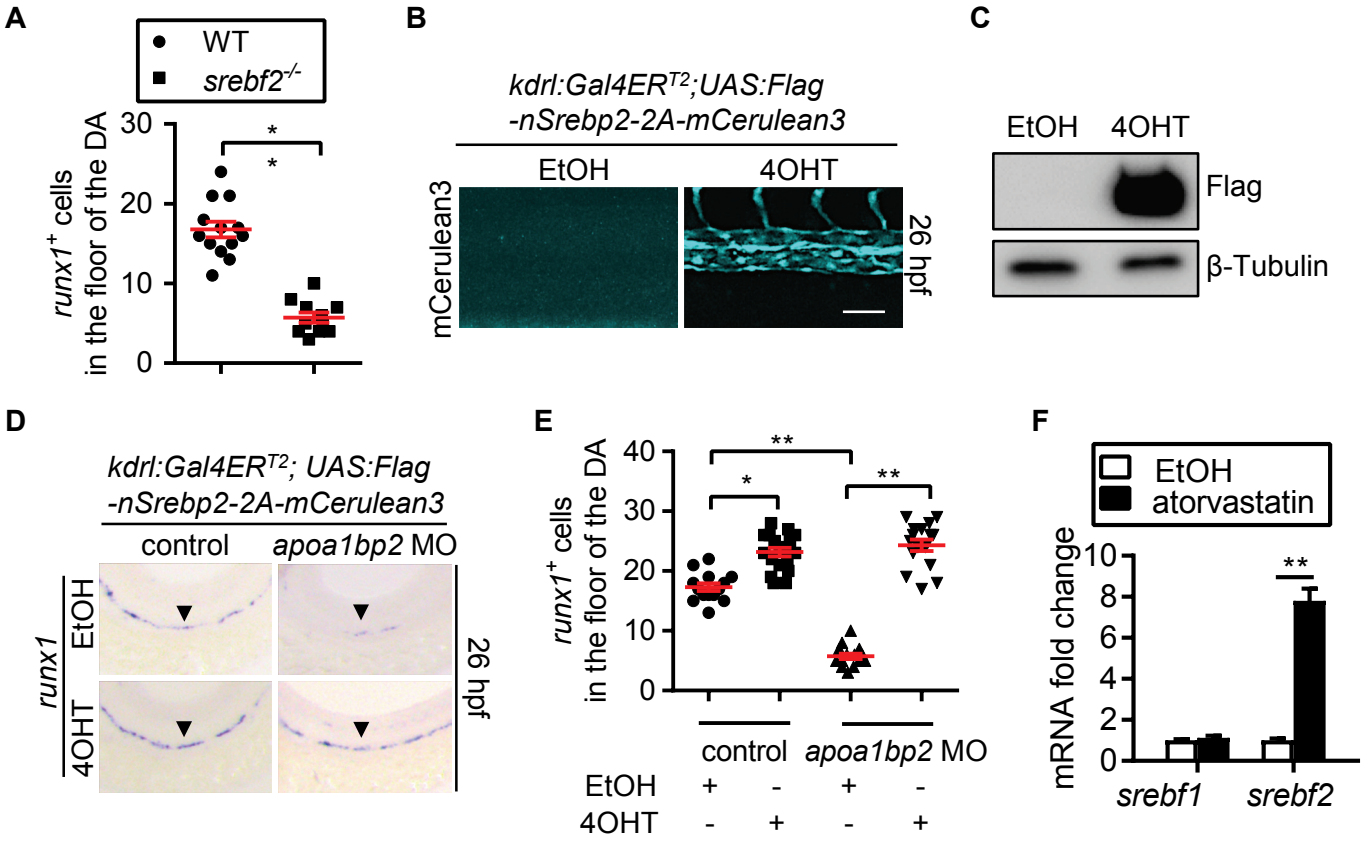

Fig. S11. Srebp2 deficiency impairs HSC emergence. A. Quantification of *runx1*$^{+}$ HSCs in the floor of DA in **Fig. 3A**. **B.** mCerulean3 signals at 26 hpf in *kdrl:Gal4ER*^{T2}*; UAS:Flag-nSrebp2-2A-mCerulean3* embryos treated with EtOH or 4OHT (6-26 hpf). **C.** Immunoblotting of Srebp2 expression in embryos from panel **B**. **D**. WISH analysis of *runx1* expression in control or Aibp2-deficient zebrafish treated with control vehicle or 4OHT. **E**. Quantification of *runx1*$^{+}$ HSCs in the floor of DA in **D**. **F**. WT zebrafish were treated with EtOH or atorvastatin from 6 to 26 hpf, total RNA isolated, and qRT-PCR performed for *srebf1* and *srebf2*. Arrowheads in **D** indicate location of DA. Mean±SE; *p<0.05; **p<0.01. Scale bar: 100 μm.

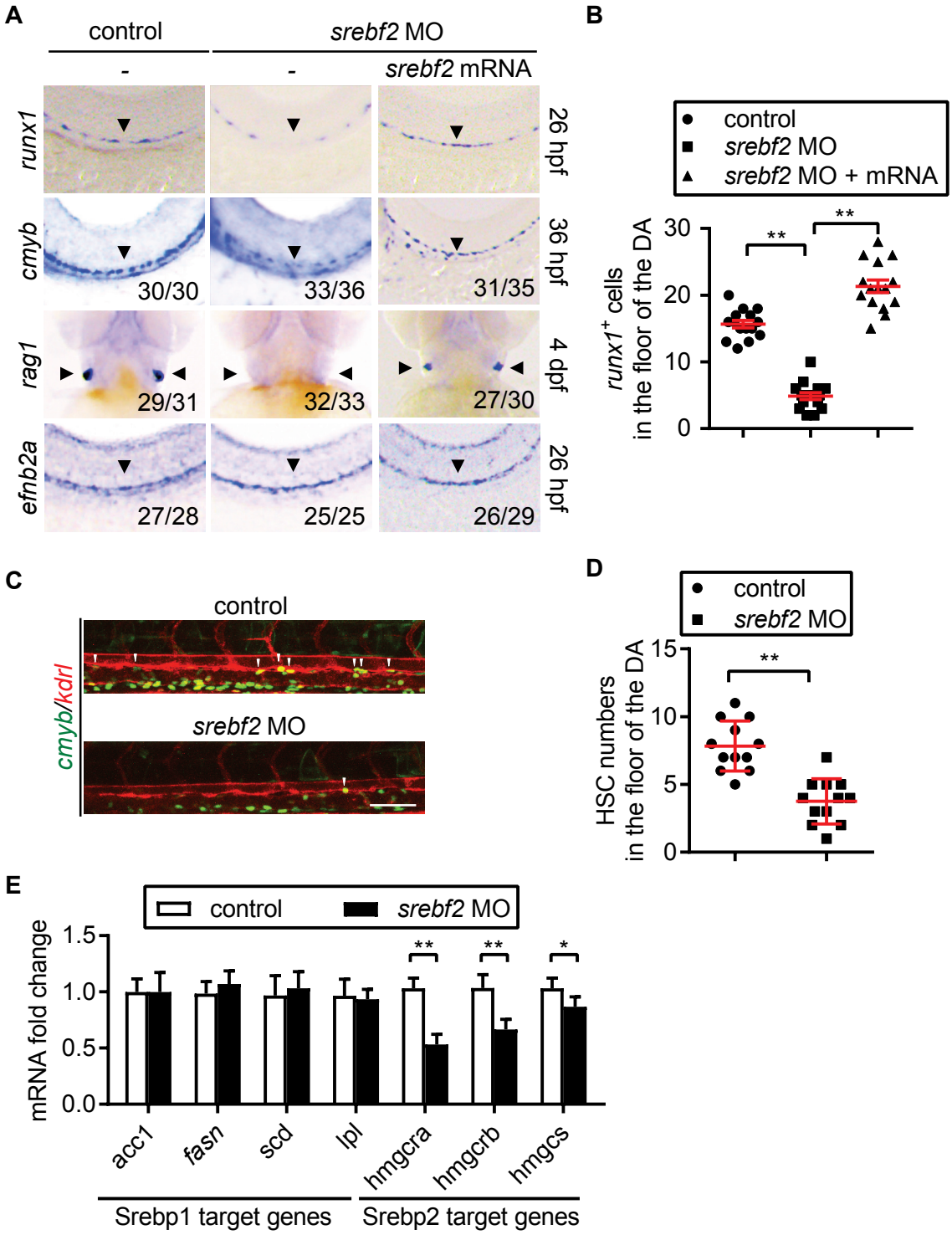

Fig. S12. Srebp2 knockdown impairs HSC emergence and its target gene expression.
A. Expression of *runx1*, *cmyb*, *rag1*, and *efnb2a* in control or Srebp2 knockdown animals at the indicated time. Arrowheads indicate DA or thymus. **B.** Quantitative data of *runx1*$^{+}$ HSCs in panel **A**. **C.** Confocal imaging of *cmyb*$^{+}$*kdrl*$^{+}$ HSCs in the floor of the DA of control or Srebp2-deficient animals. Arrowheads show *cmyb*$^{+}$*kdrl*$^{+}$ HSCs in the floor of DA. **D.** The quantitative data of panel **C**. **E.** Quantitative RT-PCR analysis of Srebp1 and Srebp2 downstream gene expression in control or Srebp2 knockdown animals. Mean±SE; *p<0.05; **p<0.01; scale bar: 100 μm.

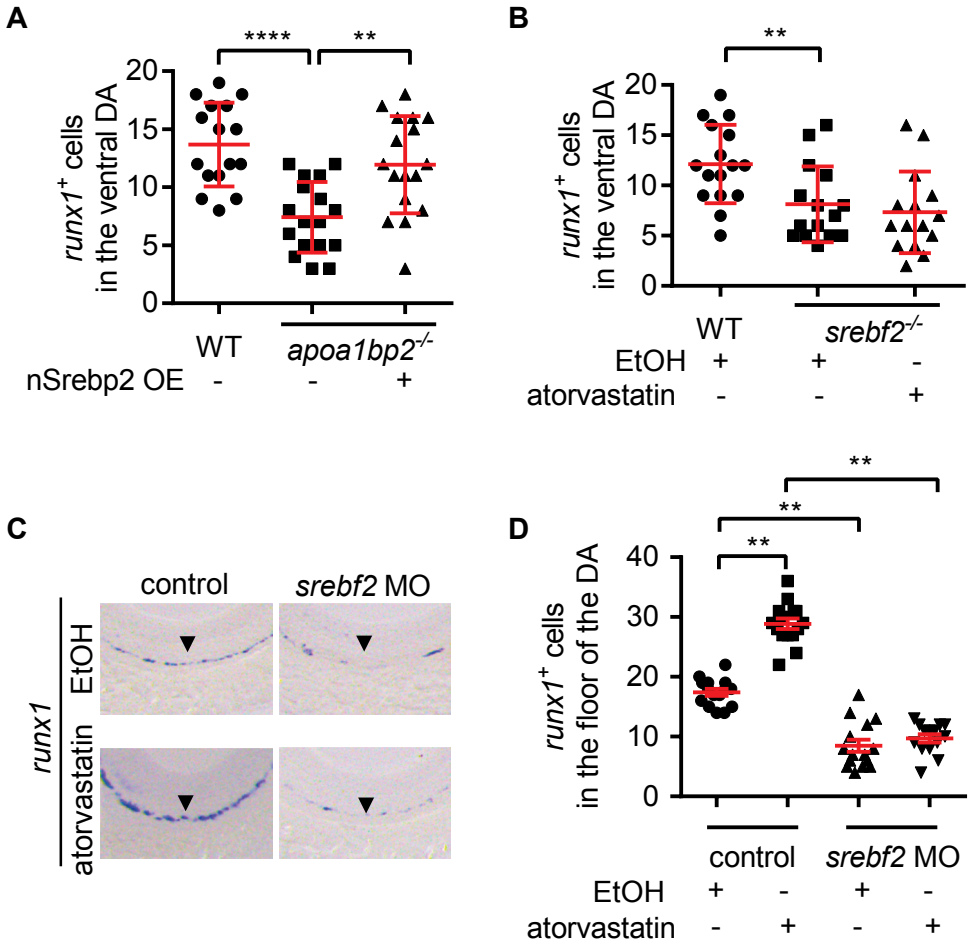

Fig. S13. The atorvastatin effect on HSC specification is dependent on Srebp2. A and **B.** Quantification of HSC in the floor of DA in **Fig. 3B** (**A**) and **Fig. 3C** (**B**). **C.** The expression of *runx1* in control or *srebf2* morphants treated with EtOH or 1 μM atorvastatin. **D.** The quantitative data of *runx1*$^{+}$ HSCs in the floor of DA in panel **C**. Arrowheads in **C** indicate location of DA. Mean±SE; **p<0.01; ****p<0.0001.

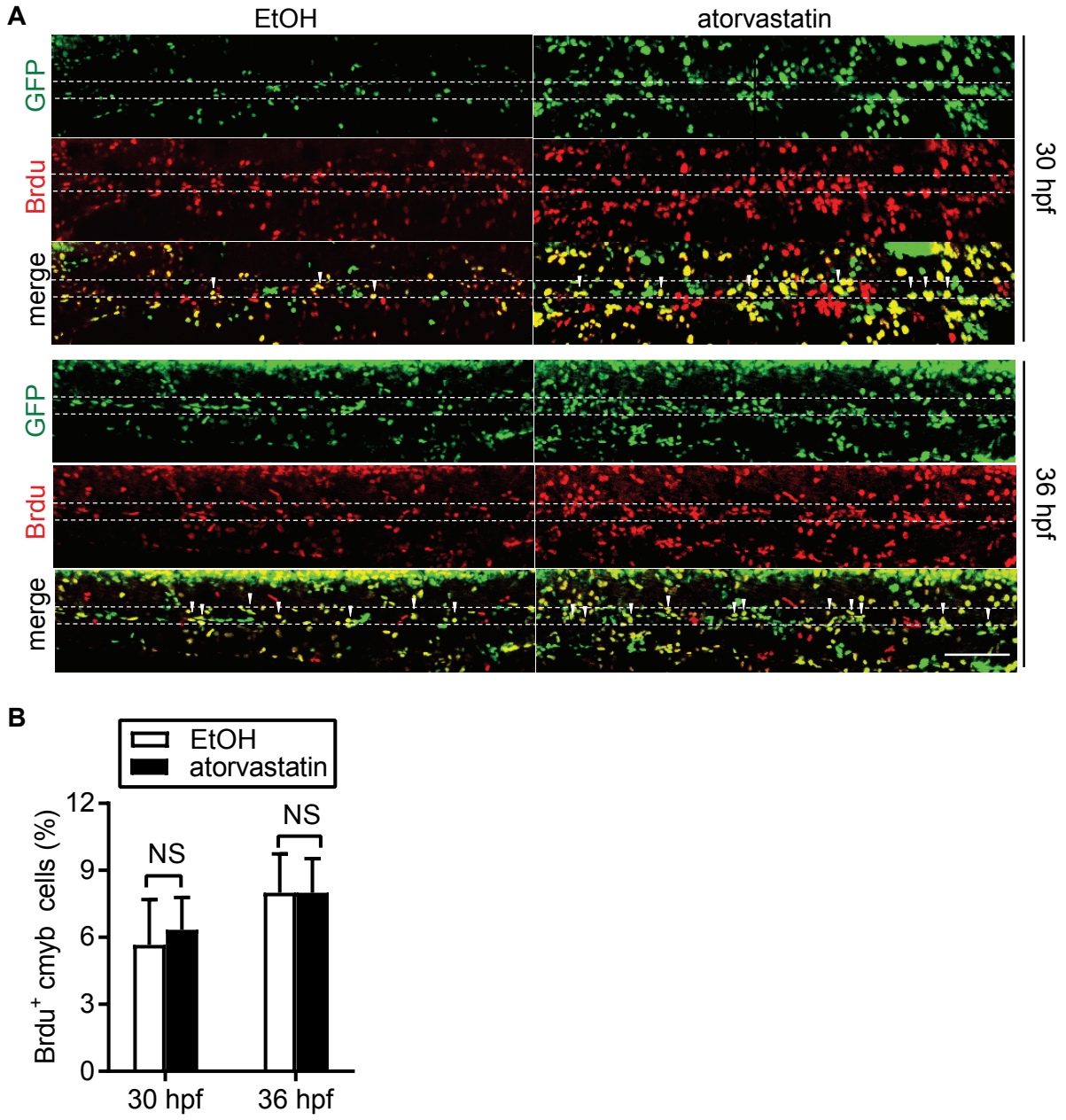

Fig. S14. Increased HSC emerge by atorvastatin treatment is not due to hyperproliferation. A. The *cmyb:GFP* zebrafish embryos were treated with atorvastatin or EtOH control (6-30 or 6-36 hpf), and Brdu incorporation into proliferating cells assessed by confocal microscopy. The two white dash lines indicate DA. Merged yellow signals show proliferating *cmyb*$^{+}$ cells. Arrowheads indicate proliferating HSPCs. **B.** Quantitative data of proliferating *cmyb*$^{+}$ cells at 30 and 36 hpf. Arrowheads show the proliferating *cmyb*$^{+}$ HSPCs in the floor of the DA of EtOH or atorvastatin-treated animals. Mean±SE; NS: not significant. Scale bar: 100 μm.

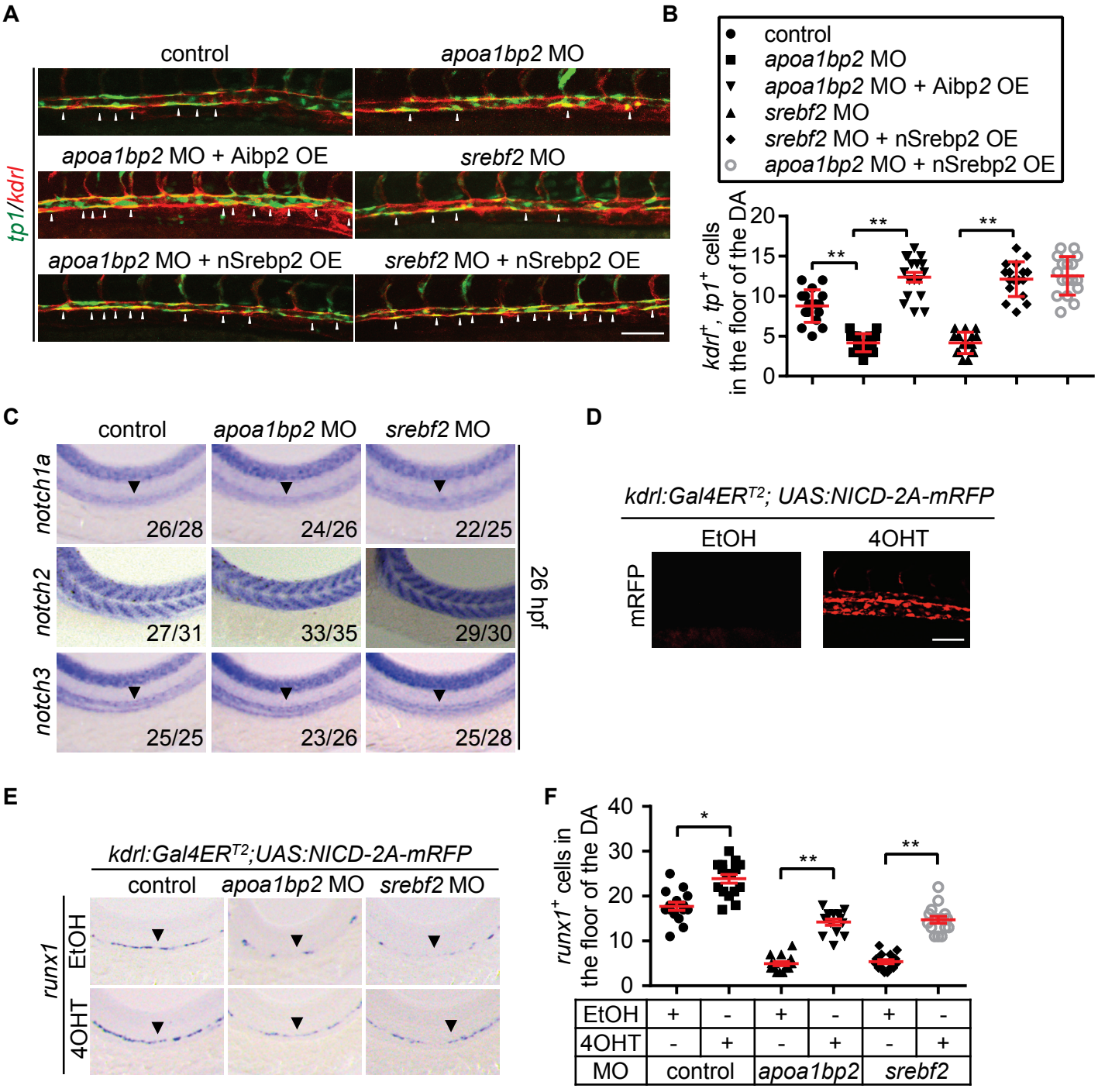

Fig. S15. A. Effects of *apoa1bp2* and *srebf2* deficiency on Notch signaling. A. The EGFP signal in the DA of 28 hpf *tp1:d2GFP; kdrl:mCherry* embryos injected with the indicated MOs, with or without Aibp2 or nSrebp2 (N-terminal 460aa) mRNA overexpression (OE). Arrowheads denote HSPCs in the floor of the DA with active Notch signaling. **B.** Quantification of *tp1*$^{+}$*kdrl*$^{+}$ HSPCs in panel **A**. OE: overexpression. **C.** WISH analyses of *notch1a, notch2,* and *notch3* in Aibp2-, Srebp2-deficient or control animals. Arrowheads show DA. **D.** The mRFP signals in 26 hpf *kdrl:Gal4ER*^{T2}*; UAS:NICD-2A-mRFP* embryos treated with EtOH or 4OHT (6-26 hpf). **E.** The expression of *runx1* in the DA of the indicated zebrafish. Arrowheads indicate DA. **F.** Quantification of *runx1*$^{+}$ HSCs in the floor of DA in panel **E**. Mean±SE; *p<0.05; **p<0.01. Scale bar: 100 μm.

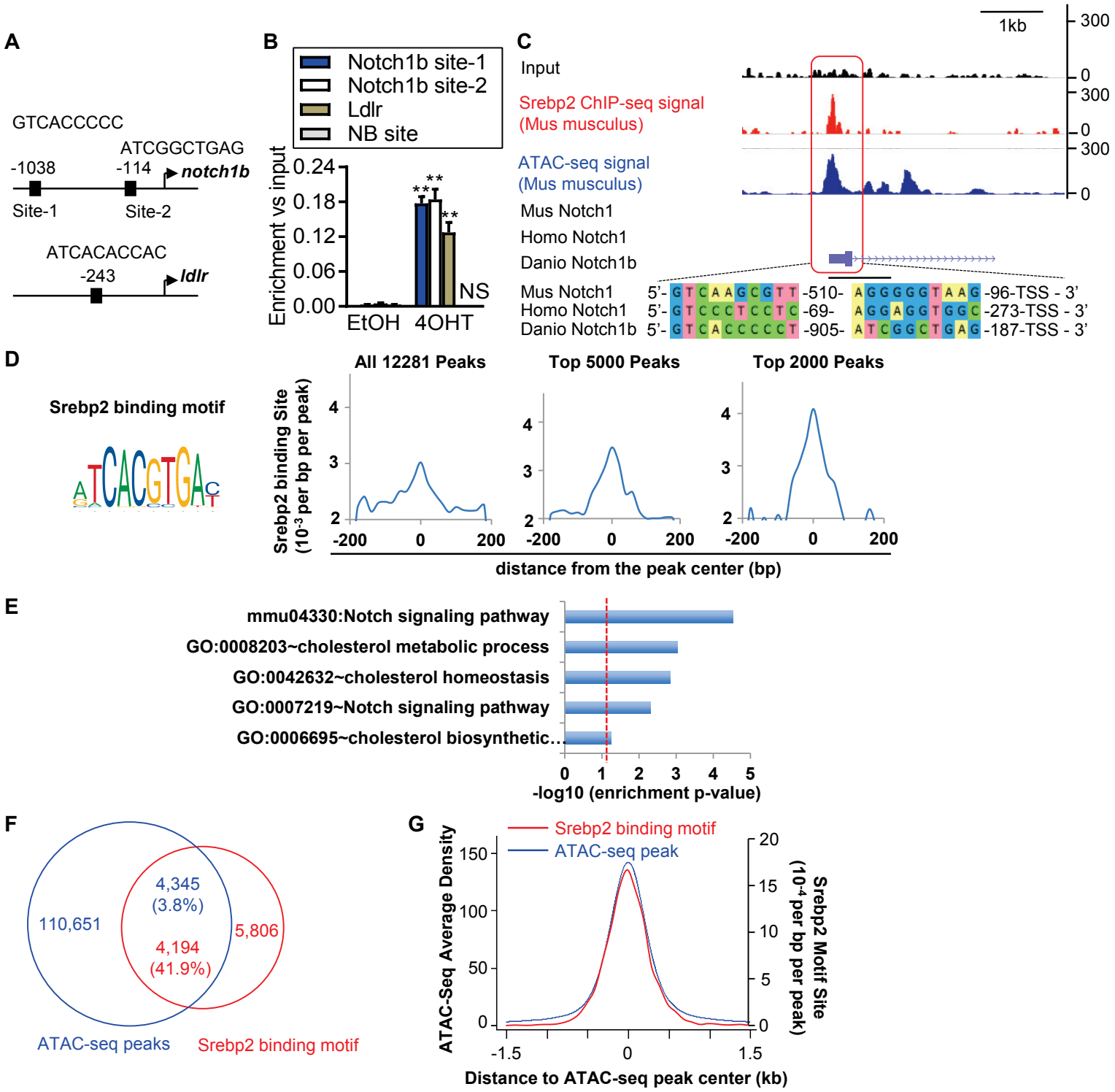

Fig. S16. Bioinformatics analysis of Srebp2 regulation of the Notch pathway. A. Predicted Srebp2 binding sites on *notch1b* and *ldlr* promoters by JASPAR. **B.** Promoter occupancy of the *notch1b*, *ldlr,* or non-binding (NB) site within *notch1b* intron. The *kdrl:Gal4ER*^{T2}*; UAS:Flag-nSrebp2-2A-mCerulean3* embryos were treated with EtOH or 4OHT from 6 to 26 hpf, ChIP assays were performed with an anti-Flag antibody, and qPCR conducted as indicated. **C**. Representative Srebp2 binding peaks on Notch1 promoter in mice. Bioinformatics analysis also identified similar Srebp2 binding motifs in human and zebrafish Notch1 genes. The numbers indicate distance between the two motifs. **D.** Average enrichment of Srebp2 binding motif towards the center of Srebp2 ChIP-seq peaks calculated with increasing stringency from left to right. **E.** Gene Ontology and KEGG pathway enrichment analyses reveal that genes with Srebp2 binding motif in their promoters are associated with the Notch pathway and cholesterol metabolism. Red line marks the value of p=0.05. **F.** Venn diagram showing the overlap between regions of ATAC-seq peaks and regions containing Srebp2 binding motif. **G.** Srebp2 binding motif enrichment in ATAC-seq peaks. Average density plots of ATAC-seq (left y-axis) and average enrichment of Srebp2 binding motif (right y-axis) ±1.5 kb to the center of ATAC-seq peaks. Mean±SE; **p<0.01; NS: not significant.

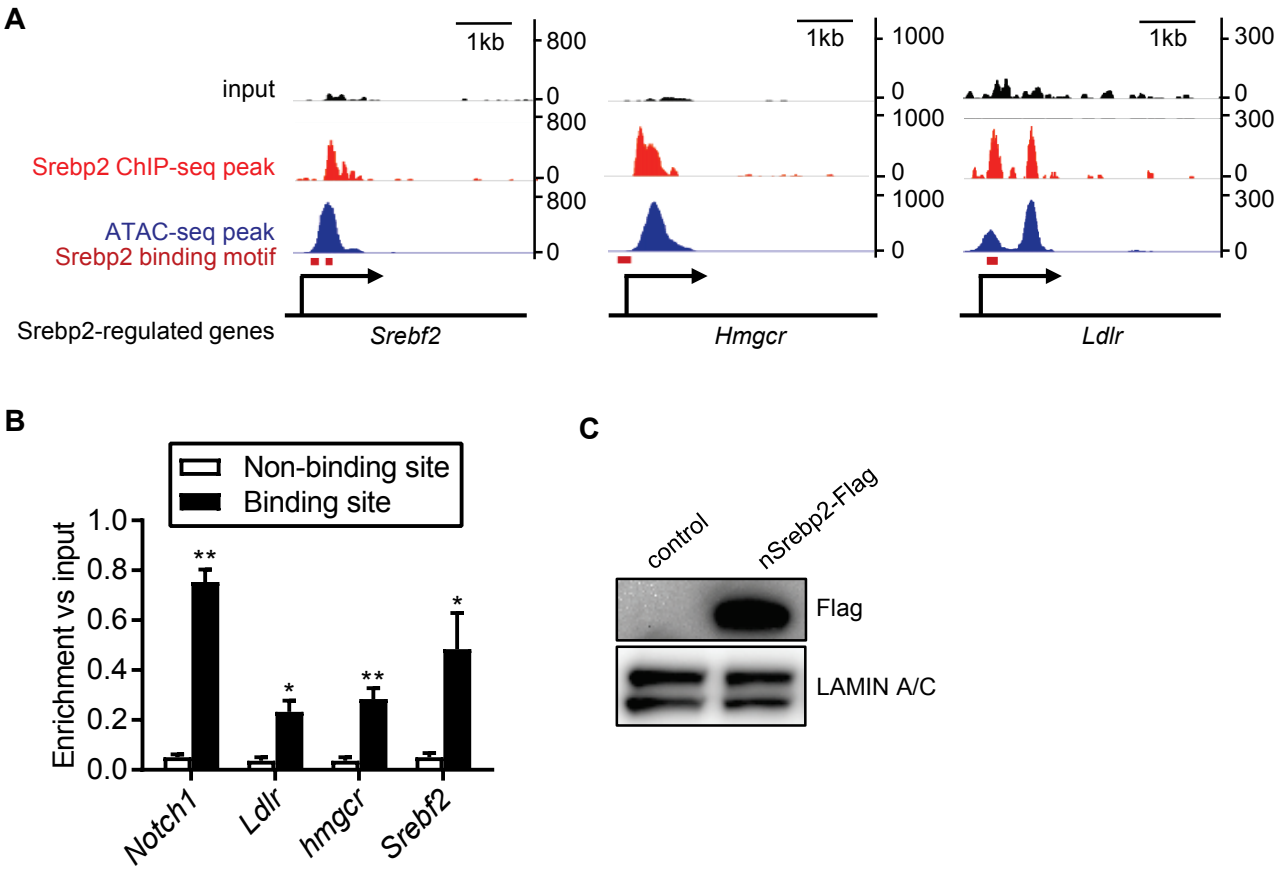

Fig. S17. Experimental validation of Srebp2 regulation of Notch pathway. A. Locations of Srebp2 ChIP-Seq peaks, ATAC-seq peaks and Srebf2 binding motifs are highlighted on the promoters of canonical Srebp2-regulated genes *Srebf2*, *Hmgcr*, and *Ldlr*. **B.** Validation of Srebp2 binding to its putatively regulated genes (*Ldlr*, *Hmgcr*, and *Srebf2*) and Notch1. Mouse ECs were infected with Lenti-nSrebp2-Flag. The infected cells were selected using puromycin for 1 month to establish stably nSrebp2-expressing cells, which were fixed and ChIP performed using an anti-Flag antibody, and qPCR conducted using primers listed in **materials and methods**. **C**. Immunoblotting of overexpressed active nuclear Srebp2 (nSrebp2), with LAMIN A/C serving as the loading control. Mean±SE; *p<0.05; **p<0.01.

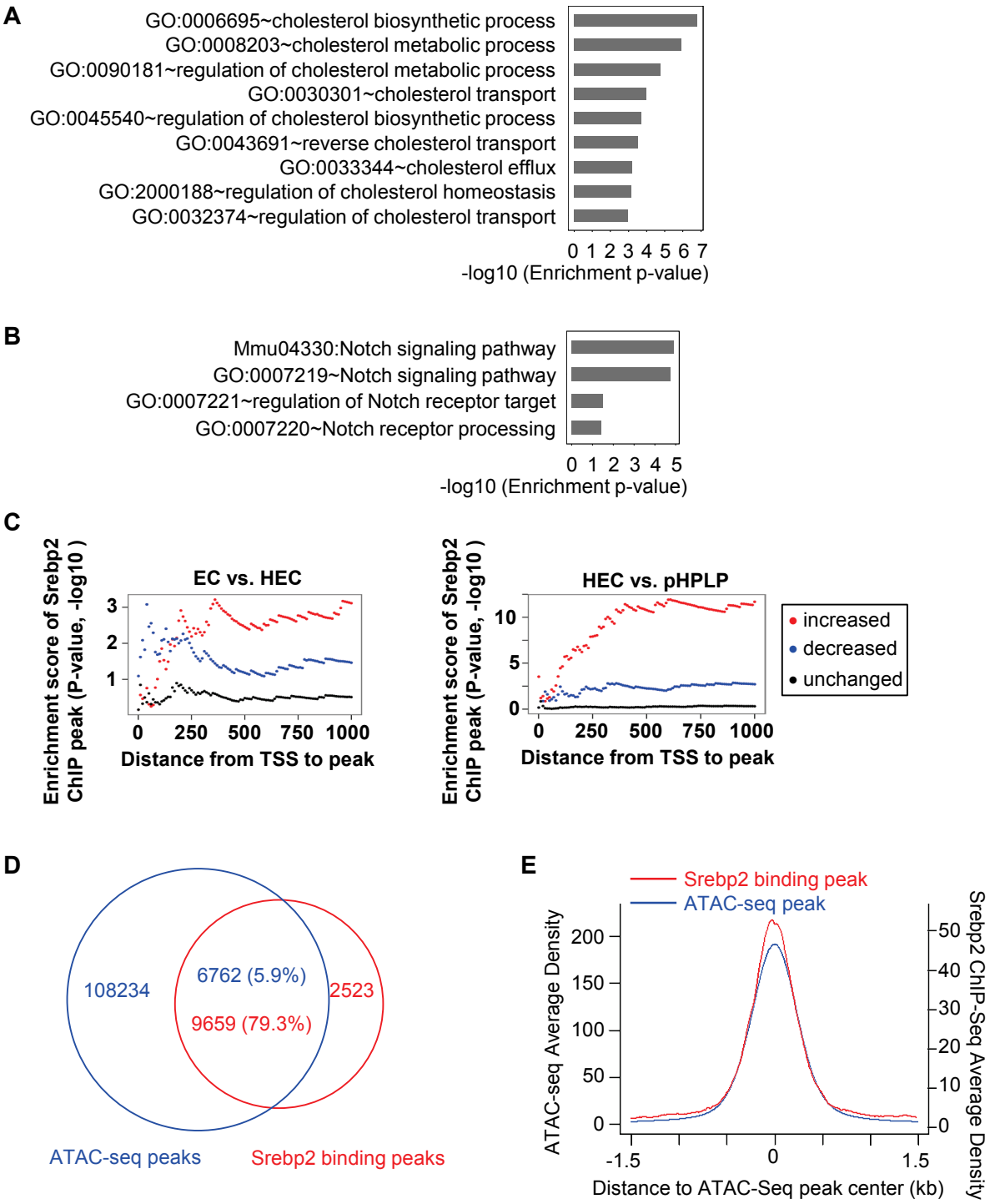

Fig. S18. Bioinformatics analysis and experimental validation of Srebp2 regulation of Notch pathway. Gene Ontology and KEGG pathway enrichment analyses show that Srebp2-bound genes are associated with the Notch pathway (**A**) and cholesterol metabolism (**B**). **C.** Mann–Whitney U test of p-value of Srebp2 binding peak enrichment (y-axis) in differentially expressed genes. X-axis represents the range of peak association cutoffs as measured by distances between translation start site (TSS) and Srebp2 binding peak in an individual gene. **D**. Venn diagram illustrating 79.3% of overlap between ATAC-seq peaks (blue) and Srebp2 binding peaks (red). **E.** Srebp2 binding peaks overlap ATAC-seq peaks. Average density plots of ATAC-seq (left y-axis) and Srebp2 ChIP-seq (right y-axis) ±1.5 kb to the center of ATAC-Seq peaks.

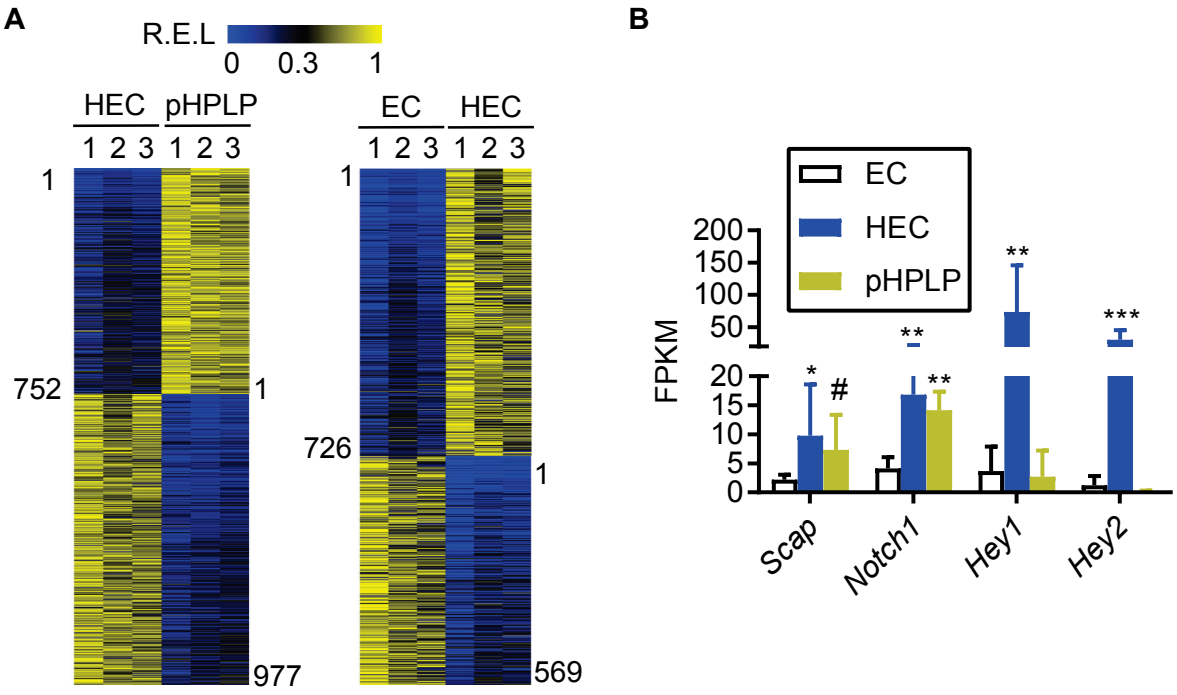

Fig. S19. Bioinformatics analysis of public RNA-seq data. A. Heat maps of relative expression levels (R.E.L) of genes in isolated ECs, HECs, and pre-HSCs and progenitors with lymphoid potential (pHPLP). **B.** The mRNA levels of the indicated genes in the public RNA-seq dataset. FPKM: fragments per kilobase of transcript per million mapped reads. The p value was calculated using negative binomial test. Mean±SD; n=3. #, p=0.08. *p<0.05; **p<0.01; ***p<0.001.

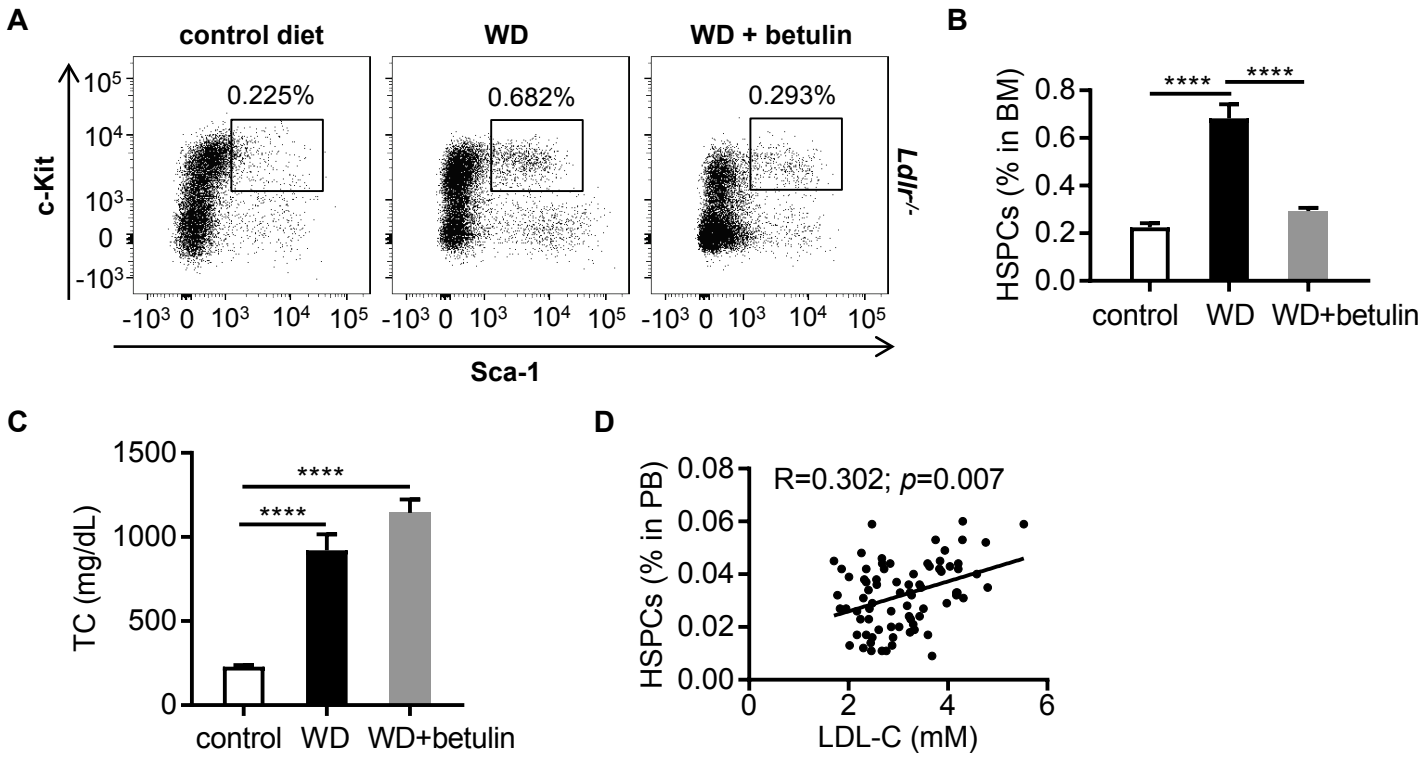

Fig. S20. **Hypercholesterolemia effect on HSPC expansion. A.** FACS analysis of Lin$^-$Sca-1$^+$c-Kit$^+$ HSPCs. Eight week-old male LDLR knockout mice were fed control diet, Western diet (WD), or WD in combination with betulin (600 mg/kg food) for 16 weeks, and bone marrow were isolated from these hypercholesterolemic mice for FACS analysis of Lin$^-$Sca-1$^+$c-Kit$^+$ HSPCs. **B.** Quantitative FACS data of HSPCs in panel **A**. **C.** Total plasma cholesterol (TC) measurements. n=10 per group. **D.** The correlation of CD34$^+$CD45$^+$ HSPC frequency with LDL-C levels in normal volunteers. Mean±SE; ****p<0.0001.

Table S1a. The cholesterol metabolism-associated genes that contain Srebp2 binding motif

ABCA1
ABCA12
ABCA5
ABCA7
ABCG1
ABCG2
ABCG3
ABCG4
ABCG5
ABCG8
ADIPOQ
APOA1
APOA2
APOA4
APOA5
APOB
APOC2
APOE
APOF
APOM
CAV1
CD36
CES1D
CFTR
COMMD1
CYB5R3
CYP51
DHCR24
DHCR7
EBP
EGF
ERLIN1
ERLIN2
FDFT1
FDPS
FGF1
G6PDX
GM9745
GPS2
HMGCR
HMGCS1
HMGCS2

HSD17B7
IDI2
INSIG1
INSIG2
IRAK1
LAMTOR1
LDLR
LRP1
LSS
MVD
MVK
NFKBIA
NPC1
NPC1L1
NPC2
NR1H2
NR1H3
NSDHL
PEX2
PLA2G10
PLTP
PMVK
PON1
POR
PRKAA1
PRKAA2
PTCH1
SC5D
SCAP
SCARB1
SCP2
SEC14L2
SHH
SIRT1
SOAT1
SOAT2
SOD1
SREBF1
SREBF2
STARD4
STARD5
STX12
TM7SF2

WASHC1

Table S1b. Cholesterol biosynthesis genes that contain Srebp2 binding motif

MGI:MGI:107592	Hmgcs1	3-hydroxy-3-methylglutaryl-Coenzyme A synthase 1
MGI:MGI:107606	Srebf1	sterol regulatory element binding transcription factor 1
MGI:MGI:1913363	Apoa5	apolipoprotein A-V
MGI:MGI:1915853	Pmvk	phosphomevalonate kinase
MGI:MGI:95515	Fgf1	fibroblast growth factor 1
MGI:MGI:2387613	Erlin1	ER lipid raft associated 1
MGI:MGI:101939	Hmgcs2	3-hydroxy-3-methylglutaryl-Coenzyme A synthase 2
MGI:MGI:1336173	Prkaa2	protein kinase, AMP-activated, alpha 2 catalytic subunit
MGI:MGI:1336155	Lss	lanosterol synthase
MGI:MGI:1920416	Tm7sf2	transmembrane 7 superfamily member 2
MGI:MGI:2685089	Npc1l1	NPC1 like intracellular cholesterol transporter 1
MGI:MGI:3704398	Gm9745	predicted gene 9745
MGI:MGI:107624	Mvk	mevalonate kinase
MGI:MGI:98351	Sod1	superoxide dismutase 1, soluble
MGI:MGI:1922004	Dhcr24	24-dehydrocholesterol reductase
MGI:MGI:2148202	Ces1d	carboxylesterase 1D
MGI:MGI:2135958	Scap	SREBF chaperone
MGI:MGI:1298378	Dhcr7	7-dehydrocholesterol reductase
MGI:MGI:107822	Ebp	phenylalkylamine Ca2+ antagonist (emopamil) binding protein
MGI:MGI:107486	Pex2	peroxisomal biogenesis factor 2
MGI:MGI:2387215	Erlin2	ER lipid raft associated 2
MGI:MGI:94893	Cyb5r3	cytochrome b5 reductase 3
MGI:MGI:104888	Fdps	farnesyl diphosphate synthetase
MGI:MGI:96159	Hmgcr	3-hydroxy-3-methylglutaryl-Coenzyme A reductase
MGI:MGI:105979	G6pdx	glucose-6-phosphate dehydrogenase X-linked
MGI:MGI:2145955	Prkaa1	protein kinase, AMP-activated, alpha 1 catalytic subunit
MGI:MGI:1915065	Sec14l2	SEC14-like lipid binding 2
MGI:MGI:88388	Cftr	cystic fibrosis transmembrane conductance regulator
MGI:MGI:102706	Fdft1	farnesyl diphosphate farnesyl transferase 1
MGI:MGI:106040	Cyp51	cytochrome P450, family 51
MGI:MGI:1916289	Insig1	insulin induced gene 1
MGI:MGI:88057	Apoe	apolipoprotein E
MGI:MGI:88052	Apob	apolipoprotein B
MGI:MGI:88051	Apoa4	apolipoprotein A-IV
MGI:MGI:88049	Apoa1	apolipoprotein A-I
MGI:MGI:1099438	Nsdhl	NAD(P) dependent steroid dehydrogenase-like
MGI:MGI:1330808	Hsd17b7	hydroxysteroid (17-beta) dehydrogenase 7
MGI:MGI:98254	Scp2	sterol carrier protein 2, liver
MGI:MGI:1353611	Sc5d	sterol-C5-desaturase
MGI:MGI:2444315	Idi2	isopentenyl-diphosphate delta isomerase 2
MGI:MGI:2179327	Mvd	mevalonate (diphospho) decarboxylase
MGI:MGI:97744	Por	P450 (cytochrome) oxidoreductase
MGI:MGI:1920249	Insig2	insulin induced gene 2
MGI:MGI:107704	Abcg1	ATP binding cassette subfamily G member 1

Table S1c. Cholesterol efflux genes that contain Srebp2 binding motif

MGI:MGI:107585	Srebf2	sterol regulatory element binding factor 2
MGI:MGI:1913363	Apoa5	apolipoprotein A-V
MGI:MGI:106675	Adipoq	adiponectin, C1Q and collagen domain containing
MGI:MGI:1097712	Npc1	NPC intracellular cholesterol transporter 1
MGI:MGI:95290	Egf	epidermal growth factor
MGI:MGI:103151	Pltp	phospholipid transfer protein
MGI:MGI:2386607	Abca5	ATP-binding cassette, sub-family A (ABC1), member 5
MGI:MGI:1915213	Npc2	NPC intracellular cholesterol transporter 2
MGI:MGI:1930124	Apom	apolipoprotein M
MGI:MGI:2135607	Sirt1	sirtuin 1
MGI:MGI:1891751	Gps2	G protein pathway suppressor 2
MGI:MGI:104539	Apof	apolipoprotein F
MGI:MGI:96828	Lrp1	low density lipoprotein receptor-related protein 1
MGI:MGI:1890594	Abcg4	ATP binding cassette subfamily G member 4
MGI:MGI:1332226	Soat2	sterol O-acyltransferase 2
MGI:MGI:88054	Apoc2	apolipoprotein C-II
MGI:MGI:1347061	Abcg2	ATP binding cassette subfamily G member 2 (Junior blood group)
MGI:MGI:107420	Irak1	interleukin-1 receptor-associated kinase 1
MGI:MGI:104665	Soat1	sterol O-acyltransferase 1
MGI:MGI:99607	Abca1	ATP-binding cassette, sub-family A (ABC1), member 1
MGI:MGI:1914720	Abcg8	ATP binding cassette subfamily G member 8
MGI:MGI:103295	Pon1	paraoxonase 1
MGI:MGI:105373	Ptch1	patched 1
MGI:MGI:2676312	Abca12	ATP-binding cassette, sub-family A (ABC1), member 12
MGI:MGI:102709	Cav1	caveolin 1, caveolae protein
MGI:MGI:893578	Scarb1	scavenger receptor class B, member 1
MGI:MGI:88057	Apoe	apolipoprotein E
MGI:MGI:88052	Apob	apolipoprotein B
MGI:MGI:88051	Apoa4	apolipoprotein A-IV
MGI:MGI:88050	Apoa2	apolipoprotein A-II
MGI:MGI:88049	Apoa1	apolipoprotein A-I
MGI:MGI:104741	Nfkbia	nuclear factor of kappa light polypeptide gene enhancer in B cells inhibitor, alpha
MGI:MGI:98297	Shh	sonic hedgehog
MGI:MGI:1352463	Nr1h2	nuclear receptor subfamily 1, group H, member 2
MGI:MGI:1352462	Nr1h3	nuclear receptor subfamily 1, group H, member 3
MGI:MGI:1347522	Pla2g10	phospholipase A2, group X
MGI:MGI:1931027	Stx12	syntaxin 12
MGI:MGI:1913758	Lamtor1	late endosomal/lysosomal adaptor, MAPK and MTOR activator 1
MGI:MGI:1351659	Abcg5	ATP binding cassette subfamily G member 5
MGI:MGI:1351646	Abca7	ATP-binding cassette, sub-family A (ABC1), member 7
MGI:MGI:1351624	Abcg3	ATP binding cassette subfamily G member 3
MGI:MGI:107704	Abcg1	ATP binding cassette subfamily G member 1

Table S1d. Cholesterol uptake genes that contain Srebp2 binding motif

MGI:MGI:96765	Ldlr	low density lipoprotein receptor
MGI:MGI:107899	Cd36	CD36 molecule
MGI:MGI:109474	Commd1	COMM domain containing 1
MGI:MGI:893578	Scarb1	scavenger receptor class B, member 1
MGI:MGI:88050	Apoa2	apolipoprotein A-II
MGI:MGI:88049	Apoa1	apolipoprotein A-I
MGI:MGI:98254	Scp2	sterol carrier protein 2, liver
MGI:MGI:1913758	Lamtor1	late endosomal/lysosomal adaptor, MAPK and MTOR activator 1
MGI:MGI:2156765	Stard5	StAR-related lipid transfer (START) domain containing 5
MGI:MGI:2156764	Stard4	StAR-related lipid transfer (START) domain containing 4
MGI:MGI:1916017	Washc1	WASH complex subunit 1

Table S2. Srebp2 binding motifs are enriched in promoters of Notch pathway genes (shown in red).

DAVID Gene Name
C-terminal binding protein 1(Ctbp1)
C-terminal binding protein 2(Ctbp2)
CREB binding protein(Crebbp)
E1A binding protein p300(Ep300)
K(lysine) acetyltransferase 2A(Kat2a)
K(lysine) acetyltransferase 2B(Kat2b)
LFNG O-fucosylpeptide 3-beta-N-acetylglucosaminyltransferase(Lfng)
MFNG O-fucosylpeptide 3-beta-N-acetylglucosaminyltransferase(Mfng)
RFNG O-fucosylpeptide 3-beta-N-acetylglucosaminyltransferase(Rfng)
SNW domain containing 1(Snw1)
a disintegrin and metallopeptidase domain 17(Adam17)
aph1 homolog A, gamma secretase subunit(Aph1a)
aph1 homolog B, gamma secretase subunit(Aph1b)
aph1 homolog C, gamma secretase subunit(Aph1c)
corepressor interacting with RBPJ, 1(Cir1)
delta-like 1 (Drosophila)(Dll1)
delta-like 3 (Drosophila)(Dll3)
delta-like 4 (Drosophila)(Dll4)
deltex 1, E3 ubiquitin ligase(Dtx1)
deltex 2, E3 ubiquitin ligase(Dtx2)
deltex 3, E3 ubiquitin ligase(Dtx3)
deltex 3-like, E3 ubiquitin ligase(Dtx3l)
deltex 4, E3 ubiquitin ligase(Dtx4)
dishevelled segment polarity protein 1(Dvl1)
dishevelled segment polarity protein 2(Dvl2)
dishevelled segment polarity protein 3(Dvl3)
hairy and enhancer of split 1 (Drosophila)(Hes1)
hairy and enhancer of split 5 (Drosophila)(Hes5)
histone deacetylase 1(Hdac1)
histone deacetylase 2(Hdac2)
jagged 1(Jag1)
jagged 2(Jag2)
mastermind like 1 (Drosophila)(Maml1)
mastermind like 2 (Drosophila)(Maml2)
mastermind like 3 (Drosophila)(Maml3)
nicastrin(Ncstn)
notch 1(Notch1)
notch 2(Notch2)
notch 3(Notch3)
notch 4(Notch4)
nuclear receptor co-repressor 2(Ncor2)
numb homolog (Drosophila)(Numb)
numb-like(Numbl)
pre T cell antigen receptor alpha(Ptcra)
presenilin 1(Psen1)
presenilin 2(Psen2)
presenilin enhancer gamma secretase subunit(Psenen)
recombination signal binding protein for immunoglobulin kappa J region(Rbpj)
recombination signal binding protein for immunoglobulin kappa J region-like(Rbpjl)

Table S3a. Change of Notch pathway genes comparing HEC with EC

Gene	# of times appea	log2(Fold chang) (HEC	Diff exp P-value
JAG2	2	7.362250515	1.14E-07
HEY2	1	4.746263029	9.75E-05
HEY1	1	4.069871741	0.000104339
NOTCH4	2	5.347014595	0.000183082
NRARP	1	4.069648014	0.000204744
JAG1	2	2.362962772	0.000240383
NOTCH1	4	1.940885625	0.002655422
AKT1S1	1	3.165303671	0.006073467
RBM15	2	-2.587416137	0.009175135
HHEX	1	1.636351781	0.016751957
RFNG	2	2.82382368	0.02014869
DLK1	1	-1.709945003	0.035808479
MAML3	3	-1.945902209	0.044649966
NEURL1A	1	2.031319626	0.048199048
MMP14	1	1.270678412	0.048514294
POFUT1	1	1.432351736	0.062647205
BMP2	1	-2.262278505	0.06407152
APP	1	0.962012689	0.068188477
WDR12	1	-1.083110912	0.07672339
NFKBIA	1	1.166448359	0.096545253
AAK1	1	1.06754936	0.120146716
ZFP423	1	1.322918465	0.121315247
SNAI2	1	-1.235889379	0.15364244
PTP4A3	1	1.241701997	0.195540395
ANXA4	1	1.164331887	0.196734191
TSPAN14	1	0.66541052	0.204235584
IFT88	1	-1.333273616	0.216204875
GMDS	1	1.16651271	0.216686713
FBXW7	1	0.81963942	0.220458472
DVL1	1	1.18833712	0.231669446
HIF1AN	1	0.781202807	0.251182777
CBFA2T2	1	-0.894863737	0.251551565
IFT172	1	-1.048449517	0.283765558
CTBP2	1	0.55270453	0.315820046
NOTCH2	3	-0.762831732	0.331708358
EPN2	1	0.74253827	0.34751614
CREB1	1	-0.658827114	0.352054037
MAML2	3	0.729311802	0.397351435
RBPJ	3	-0.620409698	0.399002518
RPS27A	1	-0.90166926	0.408316225
DVL3	1	0.666404015	0.429750958
MAML1	3	0.706923888	0.450916152
MIB1	1	-0.413460627	0.453994008

EPN1	1	0.581602034	0.492295458
FOXC1	1	0.600484887	0.512860267
TSPAN15	1	0.650500101	0.515837846
NCSTN	3	0.363150355	0.523219527
CIR1	1	0.644369944	0.536016829
UBA52	1	-0.313822863	0.545182737
ADAM10	2	0.323043445	0.557691895
UBB	1	-0.306164968	0.568502202
EP300	2	0.381843742	0.621325029
UBC	1	-0.475057838	0.62507336
POGLUT1	1	-0.41981102	0.625912581
PSEN2	3	0.425590521	0.635478989
CDKN1B	1	-0.424384531	0.654610603
HDAC2	1	0.25394141	0.661346187
RPS19	1	-0.218695378	0.710642663
GOT1	1	-0.261127946	0.722561681
NOTCH3	2	0.290447844	0.729789839
NCOR2	1	0.355122387	0.741319204
KAT2B	2	0.312498847	0.770603122
CTBP1	1	0.179242603	0.785423065
KAT2A	1	0.200850154	0.794444433
NLE1	1	0.2150448	0.794514474
APH1C	3	0.247053013	0.823824328
HDAC1	1	0.144010226	0.828560556
SEL1L	1	-0.085195518	0.882046495
GALNT11	2	0.1576658	0.898964415
HES1	2	0.062471624	0.940714588
SORBS2	1	0.064725343	0.953648761
CREBBP	1	0.026316577	0.967616258

Table S3b. Change of cholesterol metabolism pathway genes comparing HEC with EC

Gene	# of times appear	log2(Fold chang) (HEC/EC)	Diff exp P-value
SEC14L2	8	4.957678406	0.000152535
PLTP	7	2.769841564	0.014974845
EIF2AK3	2	2.132574152	0.098102653
SCAP	**6**	**2.022933346**	**0.038697685**
APLP2	2	2.02107539	0.002894879
RALY	1	1.684979016	0.058350608
STARD4	6	1.553754438	0.013892637
ARHGEF10L	2	1.381938812	0.179991713
NFKBIA	7	1.166448359	0.096545253
LRP5	4	1.139912845	0.30632407
LDLRAP1	8	1.100952011	0.333015644
APP	2	0.962012689	0.068188477
SREBF2	8	0.954528475	0.273842756
EBPL	1	0.832745415	0.473021039
PRKAA1	4	0.830777528	0.387830374
FBXW7	2	0.81963942	0.220458472
OSBP	1	0.768200332	0.329734869
PLSCR3	2	0.751204346	0.370117245
NUS1	7	0.694701287	0.275488583
FDX1	2	0.690024546	0.526056943
IRAK1	5	0.628618136	0.307646993
CYB5R3	4	0.619989322	0.23681679
ACADL	1	0.545544675	0.46967596
DHCR24	4	0.542961152	0.405182987
NCOR1	2	0.542291146	0.302325299
ALMS1	2	0.48740096	0.652327938
POR	8	0.486876484	0.512549867
CAT	2	0.464983481	0.373108116
NPC1	8	0.437729869	0.557767297
MVD	4	0.405492969	0.572167642
FDFT1	4	0.394481456	0.496915235
MVK	4	0.364316493	0.602610088
LIPA	1	0.350428871	0.612735015
SOD1	6	0.338524657	0.51289941
STARD5	4	0.329371511	0.730176194
SEC24A	3	0.271346949	0.727191154
VPS4A	4	0.25986533	0.745719666
SC5D	4	0.237845855	0.656300252
SQLE	3	0.214361107	0.706041565
CYP51	4	0.185378835	0.764991409
XBP1	2	0.142430776	0.831781214
MBTPS1	2	0.115683538	0.851831641
HSD17B7	4	0.090373003	0.919523692
LRP6	4	0.084075594	0.899726308

STX12	3	0.061889461	0.908238917
APOE	16	0.005023259	0.996350352
SCARB1	10	-0.045157175	0.94074908
NPC2	9	-0.05562968	0.908456359
ACAT2	6	-0.09654719	0.856116033
DHCR7	6	-0.111301831	0.858267132
PMVK	4	-0.149656334	0.803094631
INSIG1	6	-0.173820112	0.797948061
MED13	2	-0.222971652	0.707502184
LMF1	1	-0.240658231	0.773841754
HMGCR	4	-0.249345503	0.650411767
SCP2	18	-0.254876954	0.70441867
FDPS	8	-0.260892245	0.708450484
ERLIN1	8	-0.272660412	0.721968556
ABCA1	14	-0.279572895	0.720927232
FECH	2	-0.284983708	0.789067383
ABCG1	20	-0.317942766	0.685570066
EHD1	2	-0.318765233	0.629343315
ERLIN2	8	-0.364362147	0.569132555
NR1H2	10	-0.404516851	0.662920119
EBP	4	-0.520064875	0.429361331
LDLR	9	-0.522283001	0.454526688
SIRT1	9	-0.546444873	0.497294686
0610007P14RIK	2	-0.551977544	0.363340037
ARV1	4	-0.566855761	0.636825892
HDLBP	2	-0.589494729	0.346422617
PTCH1	7	-0.623782738	0.411315321
TMEM97	2	-0.638546632	0.312868785
EIF2A	2	-0.705841327	0.173197201
SREBF1	8	-0.799218187	0.381555969
LSS	4	-0.816420281	0.294427852
CYB5R1	2	-0.876094896	0.400451563
INSIG2	6	-0.891956344	0.390466767
LBR	2	-0.906051057	0.093598969
LMNA	2	-1.321228473	0.08537494
LIPE	2	-1.337468438	0.280230842
APOC1	7	-1.46110442	0.168217764
TM7SF2	4	-1.679981186	0.13701982

Table S3c. Change of Notch pathway genes comparing HSC with HEC

Gene	# of times	log2(Fold chang) (HSC/HEC)	Diff exp P-value
HEY2	1	-7.664878096	4.51E-11
JAG1	2	-3.523747836	6.51E-10
MMP14	1	-2.968574017	3.70E-05
HEY1	1	-5.012551728	9.93E-05
NFKBIA	1	-2.045542706	0.000964538
RBM15	2	3.358324373	0.001166669
SNAI2	1	-5.002404763	0.001215447
NOTCH4	2	-4.168139294	0.00138803
FOXC1	1	-3.859317867	0.009684347
EPN2	1	-2.455009683	0.013154724
FBXW7	1	-1.837543015	0.018832468
MAML3	3	2.425517279	0.022395731
TSPAN15	1	-2.602421872	0.037533101
WDR12	1	1.202033844	0.039746054
APP	1	-1.457760527	0.05359721
NRARP	1	-1.811837437	0.06376742
EPN1	1	-1.65348713	0.071217564
CREB1	1	1.120027491	0.073495613
NEURL1A	1	-1.626313655	0.09210213
CTBP2	1	-0.881544835	0.096807308
IFT172	1	1.650680271	0.113157794
AAK1	1	-1.038626679	0.115413266
JAG2	2	-1.493543406	0.116349968
HES1	2	-1.261942259	0.116403415
MIB1	1	0.663778627	0.178430679
POGLUT1	1	1.042667518	0.187209894
DVL3	1	-1.180860241	0.206983057
NOTCH3	2	-1.153643468	0.229959927
GMDS	1	-1.017601671	0.237874804
PTP4A3	1	0.592891664	0.238100563
CREBBP	1	0.582536032	0.268627948
ZFP423	1	-1.104472398	0.305759313
CDK6	1	1.158533029	0.326724126
NLE1	1	0.672612068	0.336412369
NCOR2	1	0.938831836	0.371796306
ADAM10	2	0.386436991	0.394827702
RPS19	1	-0.399813657	0.400633138
NOTCH1	4	-0.360352496	0.45670573
DVL1	1	-0.699321629	0.462454181
CBFA2T2	1	0.56075845	0.466038929
MAML1	3	0.585065176	0.475679722

MIB2	1	0.835879293	0.488674571
UBB	1	-0.285131458	0.518201111
TSPAN14	1	0.278186876	0.523606359
RFNG	2	0.670188041	0.569448279
ANXA4	1	-0.475622267	0.571658828
DLK1	1	-0.55502161	0.57947284
CTBP1	1	-0.282604902	0.674315458
NOTCH2	3	0.279154126	0.724523507
HDAC1	1	-0.219675586	0.728242038
KAT2A	1	0.249367128	0.730508433
AKT1S1	1	-0.347270583	0.739946249
HDAC2	1	-0.159054047	0.758382076
KAT2B	2	-0.328109901	0.771774181
POFUT1	1	-0.185761599	0.800722179
PSEN2	3	0.221795467	0.800884054
GALNT11	2	0.220465072	0.838764868
SEL1L	1	-0.095138933	0.843161444
EP300	2	0.122447226	0.864847317
RPS27A	1	0.168058518	0.884526503
UBA52	1	0.040571344	0.926528795
MAML2	3	0.06393382	0.930808356
GOT1	1	-0.047897717	0.940410533
IFT88	1	0.075158179	0.942592963
HIF1AN	1	0.040390746	0.945445429
SORBS2	1	0.074131152	0.946020819
NCSTN	3	-0.028856701	0.952293517
SPEN	1	0.051787942	0.955921127
UBC	1	0.050380158	0.963071403
CDKN1B	1	0.02447748	0.98177917
RBPJ	3	0.018820524	0.982316707
HHEX	1	-0.008717822	0.988111901

Table S3d. Change of cholesterol metabolism pathway genes comparing HSC with HEC

Gene	# of times appear in c	log2(Fold chang	Diff exp P-value
LIPE	2	2.471618202	0.064043458
LBR	2	1.42844294	0.002025063
RORA	1	1.186224185	0.341849316
PCTP	2	1.155216282	0.27988294
INSIG2	6	1.007352134	0.334807538
ALMS1	2	0.917840994	0.357434285
SEC14L2	8	0.846735038	0.479742893
ERLIN1	8	0.845674822	0.187175522
LDLRAP1	8	0.80154864	0.388220977
LDLR	9	0.694070972	0.315895876
ABCA1	14	0.671649918	0.356179966
SIRT1	9	0.624078423	0.444459786
HDLBP	2	0.505694337	0.291496181
HMGCR	4	0.45182606	0.365204046
SOD1	6	0.450537406	0.290515856
MBTPS1	2	0.446442558	0.393559978
EIF2A	2	0.400488768	0.385468947
APOE	16	0.395621153	0.635899642
SREBF1	8	0.385664213	0.691005174
SREBF2	8	0.363980973	0.599556944
POR	8	0.3214638	0.616080986
NCOR1	2	0.319125529	0.49122151
SCP2	18	0.254413603	0.685664796
ABCG1	20	0.253401706	0.759855122
LRP6	4	0.237631577	0.683672082
LRP5	4	0.180185416	0.864506808
CLN6	2	0.138022188	0.892422907
STX12	3	0.101736665	0.829665108
EHD1	2	0.085346375	0.890487334
ERLIN2	8	0.064313011	0.916160843
MED13	2	0.0190128	0.979428365
PTCH1	7	0.004830995	0.996277416
SCARB1	10	-0.036423018	0.945310266
SEC24A	3	-0.046426884	0.947410253
0610007P14RIK	2	-0.076786234	0.892260298
IRAK1	5	-0.118230669	0.834936613
VPS4A	4	-0.160348535	0.840778393
PRKAA1	4	-0.201813804	0.814121717
ACAT2	6	-0.212907633	0.710312644
CAT	2	-0.214909053	0.637983223
DHCR7	6	-0.255246238	0.687943721
ACADL	1	-0.330599756	0.658002303
LMNA	2	-0.334341864	0.722542967

LSS	4	-0.336444201	0.702477769
CYB5R3	4	-0.351852219	0.429453555
SCAP	6	-0.402670344	0.669222789
TMEM97	2	-0.454835354	0.520301743
PMVK	4	-0.457860617	0.466165183
NPC1	8	-0.532252685	0.524468398
DHCR24	4	-0.584250268	0.367285877
LMF1	1	-0.619906563	0.508841612
HSD17B7	4	-0.623061433	0.523824715
OSBP	1	-0.626682044	0.43679279
SQLE	3	-0.63294548	0.194944882
STARD5	4	-0.669530607	0.521967212
EBPL	1	-0.680438402	0.582190539
RALY	1	-0.73091694	0.364126851
NUS1	7	-0.755468313	0.209045707
INSIG1	6	-0.76573845	0.278805789
EBP	4	-0.794622839	0.270559424
APOC1	7	-0.812948951	0.461678453
NR1H2	10	-0.839447428	0.487760887
PLSCR3	2	-0.915306448	0.160425756
FDPS	8	-0.966469106	0.206667069
CYP51	4	-0.977619297	0.129316114
LIPA	1	-0.978721774	0.11343428
NR1H3	10	-1.070527866	0.410628393
STARD4	6	-1.191021125	0.044544281
FDX1	2	-1.242046983	0.304660637
NPC2	9	-1.285796001	0.004432627
SC5D	4	-1.390461924	0.012726943
FDFT1	4	-1.407917282	0.019760002
APP	2	-1.457760527	0.05359721
MVK	4	-1.564995904	0.135597686
EIF2AK3	2	-1.671004231	0.151209036
MVD	4	-1.701811923	0.043350402
FECH	2	-1.753379429	0.169300097
APLP2	2	-1.756258276	0.00088965
FBXW7	2	-1.837543015	0.018832468
NFKBIA	7	-2.045542706	0.000964538
XBP1	2	-2.05417566	0.012949342
ARHGEF10L	2	-2.472033202	0.033441641
PLTP	7	-3.021124726	0.002291993

Table S4. Characterization of the 80 qualified male volunteers.

	Total	L-LDL Group	H-LDL Group	*P*
Age(y)	45.00±10.57	44.21±10.98	45.94±10.11	0.471
BMI(cm^2/Kg)	24.68±3.61	23.82±3.05	25.75±4.04	0.103
Systolic BP(mmHg)	118.56±10.89	116.20±10.15	121.50±11.37	0.149
Diastolic BP(mmHg)	72.58±8.81	74.10±7.33	77.38±10.33	0.274
WBC（10^9/L）	6.10±1.21	5.93±1.30	6.28±1.09	0.200
Monocyte（10^9/L）	0.44±0.13	0.43±0.15	0.45±0.11	0.489
Neutrophil（10^9/L）	3.45±0.93	3.37±1.00	3.54±0.85	0.433
Lymphocyte（10^9/L)	2.01±0.49	1.95±0.54	2.09±042	0.215
BG (mM)	5.05±0.42	5.08±0.41	5.00±0.44	0.471
TC（mM）	4.99±0.98	4.30±0.52	5.81±0.70	1.07×10^{-18}
TG（mM）	2.15±1.97	1.85±1.31	2.51±2.52	0.137
HDL（mM）	1.28±0.36	1.32±0.43	1.23±0.24	0.249

*****n=79; mean±SD; low-LDL（<3.19 mM), high-LDL（≥3.19 mM）

BP: blood pressure; WBC: white blood cells; BG: blood glucose; TC: total cholesterol; TG: total triglycerides.

References and Notes

25. M. Westerfield, *The zebrafish book: a guide for the laboratory use of zebrafish (Danio rerio)*. (University of Oregon Press, 2000).
26. J.-J. Tang *et al.*, Inhibition of SREBP by a small molecule, betulin, improves hyperlipidemia and insulin resistance and reduces atherosclerotic plaques. *Cell Metab.* **13**, 44-56 (2011).
27. S. S. Gerety *et al.*, An inducible transgene expression system for zebrafish and chick. *Development* **140**, 2235-2243 (2013).
28. C. E. Burns, D. Traver, E. Mayhall, J. L. Shepard, L. I. Zon, Hematopoietic stem cell fate is established by the Notch-Runx pathway. *Genes Dev.* **19**, 2331-2342 (2005).
29. J. Bakkers *et al.*, An important developmental role for oligosaccharides during early embryogenesis of cyprinid fish. *Proc. Natl. Acad. Sci. U. S. A.* **94**, 7982-7986 (1997).
30. L.-E. Jao, S. R. Wente, W. Chen, Efficient multiplex biallelic zebrafish genome editing using a CRISPR nuclease system. *Proc. Natl. Acad. Sci. U. S. A.* **110**, 13904-13909 (2013).
31. R. Mao *et al.*, AIBP Limits Angiogenesis Through gamma-Secretase-Mediated Upregulation of Notch Signaling. *Circ. Res.* **120**, 1727-1739 (2017).
32. T. Dull *et al.*, A third-generation lentivirus vector with a conditional packaging system. *J. Virol.* **72**, 8463-8471 (1998).
33. Y. Sancak *et al.*, The Rag GTPases bind raptor and mediate amino acid signaling to mTORC1. *Science* **320**, 1496-1501 (2008).
34. Q. Gu, X. Yang, X. He, Q. Li, Z. Cui, Generation and characterization of a transgenic zebrafish expressing the reverse tetracycline transactivator. *J Genet Genomics* **40**, 523-531 (2013).
35. X. Yang *et al.*, Nucleoporin 62-like protein activates canonical Wnt signaling through facilitating the nuclear import of β-catenin in zebrafish. *Mol. Cell. Biol.* **35**, 1110-1124 (2015).
36. Q. Gu *et al.*, Genetic ablation of solute carrier family 7a3a leads to hepatic steatosis in zebrafish during fasting. *Hepatology* **60**, 1929-1941 (2014).
37. W. Kwan *et al.*, The Central Nervous System Regulates Embryonic HSPC Production via Stress-Responsive Glucocorticoid Receptor Signaling. *Cell Stem Cell* **19**, 370-382 (2016).
38. R. Espin-Palazon *et al.*, Proinflammatory signaling regulates hematopoietic stem cell emergence. *Cell* **159**, 1070-1085 (2014).
39. K. Stoletov *et al.*, Vascular lipid accumulation, lipoprotein oxidation, and macrophage lipid uptake in hypercholesterolemic zebrafish. *Circ. Res.* **104**, 952-960 (2009).
40. M. F. Diaz *et al.*, Biomechanical forces promote blood development through prostaglandin E2 and the cAMP–PKA signaling axis. *J. Exp. Med.* **212**, 665-680 (2015).
41. K. Morgan, M. Kharas, E. Dzierzak, D. G. Gilliland, Isolation of early hematopoietic stem cells from murine yolk sac and AGM. *JoVE*, (2008).

42. S. R. Amend, K. C. Valkenburg, K. J. Pienta, Murine hind limb long bone dissection and bone marrow isolation. *JoVE*, (2016).
43. L. Gao *et al.*, TopBP1 governs hematopoietic stem/progenitor cells survival in zebrafish definitive hematopoiesis. *PLoS Genet.* **11**, e1005346 (2015).
44. S. Picelli *et al.*, Tn5 transposase and tagmentation procedures for massively scaled sequencing projects. *Genome Res.* **24**, 2033-2040 (2014).
45. D. R. Sutherland, L. Anderson, M. Keeney, R. Nayar, I. Chin-Yee, The ISHAGE guidelines for CD34+ cell determination by flow cytometry. International Society of Hematotherapy and Graft Engineering. *J. Hematother.* **5**, 213-226 (1996).